Anatomical and ultrastructural study of PRAF2 expression in the mouse central nervous system

Carmen Cifuentes-Diaz, Stefano Marullo, Stéphane Doly

Anatomical and ultrastructural study of PRAF2 expression in the mouse central nervous system

Carmen Cifuentes-Diaz[1], Stefano Marullo[2] and Stéphane Doly[2].

Affiliations:

1 Institut du Fer à Moulin, INSERM UMR-S839, Université Pierre et Marie Curie, Paris 75005, France

2 Institut Cochin, INSERM U1016, CNRS UMR8104, Université Paris Descartes, Sorbonne Paris Cité, Paris 75014, France.

Correspondence should be addressed to: Stephane DOLY, Institut Cochin, Dept. Endocrinologie, Métabolisme et Cancer, 27 rue du Faubourg St-Jacques, 75014 Paris, France.

Tel:+33-1-40-51-65-51 Fax:+33-1-40-51-65-50

E-mail: stephane.doly@inserm.fr

Keywords: PRAF2, JM4, CNS, GABA(B) receptor, synapse, cilium.

Abbreviations :

10cb: 10th Cerebellar lobule
10N: dorsal motor nucleus of vagus
12N: hypoglossal nucleus
7N : facial nucleus
aca: anterior commissure anterior part
AcbC: accumbens nucleus core
AcbSh: accumbens nucleus shell
aci: anterior commissure intrabulbar part
AD: anterodorsal thalamic nucleus
Amb: ambiguus nucleus
AOV: anterior olfactory nucleus ventral part
AP: area postrema
BM: basomedial amygdaloid nucleus
BST: bed nucleus of the stria terminalis
CNS: central nervous system
Cp: corpus callosum
CPu: caudate putamen
cu: cuneate fasciculus
Cu: cuneate nucleus
DAB: diaminobenzidine
DC: dorsal cochlear nucleus
Den: dorsal endopiriform nucleus
DG: dentate gyrus
DH: dorsal horn
DR dorsal raphe nucleus
Ecu: external cuneate nucleus
EPL: external plexiform layer
ER: endoplasmic reticulum
GABA: gamma-amino butyric acid
GCL: Granule cell layer
Gi: gigantocellular reticular nucleus
Gl: glomerular layer of the olfactory bulb
GPCRs: G protein coupled receptors
Gr: gracile nucleus
GR: granular cells layer
H: hilus

Io: inferior olive
IOC: inferior olive subnucleus C
IP: Interpeduncular nucleus
LGP: lateral globus pallidus
LH: lateral hypothalamic area
LHb: lateral habenular nucleus
LM: lateral mammillary nucleus
LRt: lateral reticular nucleus
M2: secondary motor cortex
MdV: medullary reticular nucleus ventral part
Med: medial fastigial cerebellar nucleus
MePD: medial amygdaloid nucleus posterodorsal part
MG: medial geniculate nucleus
MHb: medial habenular nucleus
Mi: Mitral cell layer of the olfactory bulb
ML: molecular layer
MM: medial mammillary nucleus
MnR: median raphe nucleus
MO: medial orbital cortex
MVB: multivesicular bodies
MVePC: medial vestibular nucleus parvicellular part
Or: strata oriens
PAG: Periaqueductal gray
Par: parietal cortex
PFl: paraflocculus
Pir: Piriform cortex
PMCo: posteromedial cortical amygdaloid nucleus
Pn: pontine nuclei
PRAF2: Prenylated Rab Acceptor Family, member 2
Prl: prelimbic cortex
Pur: purkinje cells layer
PVA: paraventricular thalamic nucleus
Pyr: pyramidal cells
Rad: stratum radiatum
RER: rough endoplasmic reticulum
Rt: reticular thalamic nucleus
sm: stria medullaris thalamus
SNC: substancia nigra compacta
SNR: substantia nigra pars reticulate
Sol: Nucleus of the solitary tract
Sp5: spinal trigeminal nucleus
VCP: ventral cochlear nucleus posterior part
VH: ventral horn
VL: ventrolateral nucleus
VMH: ventromedial hypothalamic nucleus
VPM: ventral posteromedial thalamic nucleus
VTA: ventral tegmental area
Zo: zonal layer of superior colliculus

Acknowledgments :

This work was supported by grants from the Ligue Contre le Cancer, comité de l'Oise to SD; from the PIC (projets inter-équipes) to SD ; from the French Agency for AIDS Research (ANRS-09) and the Fondation pour la Recherche Médicale (Equipe FRM-2012) to SM; SM team is member of the 'Who-am-I' research consortium.

Abstract:

Prenylated Rab Acceptor Family, member 2 (PRAF2) is a four transmembrane domain protein of 19 kDa that is highly expressed in particular areas of mammalian brains. PRAF2 is mostly found in the endoplasmic reticulum (ER) of neurons where it plays the role of gatekeeper for the GB1 subunit of the $GABA_B$ receptor, preventing its progression in the biosynthetic pathway in the absence of hetero-dimerization with the GB2 subunit. However, PRAF2 can interact with several receptors and immunofluorescence studies indicate that PRAF2 distribution is larger than the ER, suggesting additional biological functions.

Here we conducted an immuno-cytochemical study of PRAF2 distribution in mouse central nervous system (CNS) at anatomical, cellular and ultra-structural levels. PRAF2 appears widely expressed in various regions of mature CNS, such as the olfactory bulbs, cerebral cortex, amygdala, hippocampus, ventral tegmental area and spinal cord. Consistent with its regulatory role of $GABA_B$ receptors, PRAF2 was particularly abundant in brain regions known to express GB1 subunits.

However, other brain areas where GB1 is expressed, such as basal ganglia, thalamus and hypothalamus, contain little or no PRAF2. In these areas GB1 subunits might reach the cell surface of neurons independently of GB2 to exert biological functions distinct from those of $GABA_B$ receptors, or be regulated by other gatekeepers. Electron microscopy studies confirmed the localization of PRAF2 in the ER, but identified previously unappreciated localizations, in mitochondria, primary cilia and sub-synaptic region. These data indicate additional modes of $GABA_B$ regulation in specific brain areas and new biological functions of PRAF2.

Introduction :

A group a structurally heterogeneous endoplasmic reticulum (ER)- or Golgi apparatus-resident proteins, known as Yips (from Ypt-interacting proteins, Ypt being the yeast equivalent of mammalian Rab GTPases), are involved in the control of ER shape and of ER to Golgi trafficking in mammalian cells. Yips interact with and regulate the cell surface export of multi transmembrane domain cargo proteins, such as G protein coupled receptors (GPCRs) or aminoacid transporters (2007; Bjork et al. 2013; Doly and Marullo 2015; Pfeffer and Aivazian 2004). Yips are classified in several families, including the 4-transmembrane domain PRAFs (Prenylated Rab Acceptor Family members), a group of 3 proteins of ≈19 kDa sharing a conserved prenylated Rab acceptor 1 (PRA1) motif that are enriched in the brain and implicated in cellular transport and vesicle trafficking (Akiduki et al. 2007; Fenster et al. 2000; Inoue et al. 2005; Koomoa et al. 2008; Lee et al. 2011).

PRAF1 (also known as PRA1, RABA1 and Yip3 in yeast) is a Golgi-resident protein, which activates the dissociation of prenylated Rabs from the GDP dissociation inhibitor GDI, thus facilitating their association with target Golgi membranes (Hutt et al. 2000). PRAF3 (also known as JWA, PRA2, ARL6IP5, addicsin, GTRAP3-18, Yip6b) was reported to delay the ER exit of the Na^+-dependent glutamate transporter Excitatory Amino-Acid Carrier 1 (EAAC1) (Akiduki and Ikemoto 2008; Lin et al. 2001). Finally, PRAF2 (also known as JM4 or Yip 6a) was found in a two-hybrid screen to interact with the carboxy-terminus of the chemokine receptor CCR5, a co-receptor of the type-1 human immunodeficiency virus (Schweneker et al. 2005).

For several years, no clear biological function was attributed to PRAF2, except its overexpression in multiple cancers (Borsics et al. 2010; Fo et al. 2006; Vento et al. 2010; Yco et al. 2013). Recently, PRAF2 was reported to interact with GB1, the ligand-binding subunit of the $GABA_B$ receptor (Doly et al. 2015). GABA (gamma-amino butyric acid) is the

principal inhibitory neuromediator of the central nervous system (CNS). Functional $GABA_B$ receptors are composed of two distinct GB1 and GB2 protomers, which are assembled within a hetero-dimer (Kaupmann et al. 1998). GB1 is retained within the ER in the absence of GB2 (Benke 2010). PRAF2 behaves as a specific GB1 gatekeeper controlling the retention of this protomer and preventing its progression into the biosynthetic pathway, GB1 being released from PRAF2 upon competitive displacement by GB2 (Doly et al. 2015). The local concentration of PRAF2, relative to that of GB1 and GB2, thus controls cell surface receptor density impacting on $GABA_B$ function in neurons.

Only partial data are available concerning PRAF2 distribution in the CNS (Koomoa et al. 2008) and functional studies *in vivo* were exclusively performed in mice following modulation of PRAF2 concentration in the ventral tegmental area (VTA) (Doly et al. 2015). Changes of PRAF2 concentration were documented during embryonic neuronal growth in culture (Doly et al. 2015), in human nervous system cancers (Borsics et al. 2010; Geerts et al. 2007; Vento et al. 2010; Yco et al. 2013) or in case of chronic alcohol intake (Enoch et al. 2013). Because of the prominent regulatory effects of PRAF2 on $GABA_B$ function and the multiple roles of this receptor in the CNS, a precise analysis of PRAF2 distribution relative to that of $GABA_B$ subunits is of major interest. In addition, in confocal immunofluorescence microscopy studies, PRAF2 was predominantly found colocalized with ER markers, whereas fractionation studies reported its presence in synaptic vesicles preparations from rat brain (Koomoa et al. 2008). Electron microscopy (EM) studies are thus necessary to determine the precise subcellular distribution of PRAF2 and appreciate potential additional functions other than that of ER gatekeeper.

Methods:

Animals. Wild type 129S2 mice (8-10 week old) used in these experiments were in a 129S2/SvPas (129S2) background (Charles River, France). Mice were maintained on a 12 light / 12 dark schedule (lights on at 8:00 am), and housed in groups of 3 to 5, in agreement with the institutional guidelines for use of animals and their care, in compliance with national and international laws and policies (Council directives no. 87-848, October 19, 1987, "Ministère de l'Agriculture et de la Forêt, Service Vétérinaire de la Santé et de la Protection Animale", agreement N° 75-974 to M.D., 75-976 to M.B.E).

Cell Culture. Human Embryonic Kidney 293 (HEK-293) cells were maintained in Dulbecco's modified Eagle's medium at 37°C in 5% CO2-enriched humidified atmosphere. Media were supplemented with 10% fetal bovine serum (FBS) and 1% Penicillin-Streptomycin.

Plasmids and transfections. PRAF2, PRAF3 and PRAF1 cDNAs were amplified by reverse PCR from mouse brain total RNA preparations and subcloned in frame into the pEGFP-N1 vector (Clontech). HEK-293 cells were transfected using GeneJuice Transfection Reagent (Novagen) according to manufacturer instructions.

Antibodies, Peptide. The following monoclonal antibodies (mAb) or polyclonal antibodies were used for immunofluorescence labeling and electron microscopy: PRAF2 antibody (ARP American Research Products, Massachusetts, USA, JM4/PRAF2, #L166), an affinity-purified rabbit polyclonal antiserum raised against amino acid residues 165-178 of PRAF2. This sequence does not produce any significant alignments with the other PRAF members or with

unrelated proteins (Protein Blast NCBI); monoclonal anti-rabbit IgG (H+L) coupled to Alexa-594 (Invitrogen, France); F(ab')2 fragment of goat-anti-rabbit IgG (H&L, Aurion, France); polyclonal biotinylated anti-rabbit IgG (Vector, Burlingame, CA). A synthetic peptide, corresponding to amino acids 165-178 of Human PRAF2 (ARP American Research Products, Massachusetts, USA, JM4/PRAF2, #L166 BS1195P) was used as PRAF2 antibody blocking peptide. The immunizing peptide at a 5:1 ratio of peptide to antibody protein (w/w) was pre-incubated two hours in PBS with the PRAF2 antibody.

Tissue preparation. Twenty-five mice under pentobarbital anesthesia (60 mg/kg) were perfused intracardially with 10 ml of 0.9% NaCl, containing 0.1% sodium nitrite followed by 50 ml of 4% paraformaldehyde in 0.1 M sodium phosphate buffer (PB), pH 7.4. Brains and spinal cords were dissected fixed overnight in the same fixative at 4°C. Transversal sections (50-µm thick) were made using a vibratome.

Light microscopy. Immunocytochemistry was performed on free-floating sections. Sections were pre-incubated for 30 min at room temperature in 0.02 M PB, pH 7.4, containing 0.9% NaCl (PBS) and 3% bovine serum albumin (PBS-BSA), then incubated for 12 h at room temperature with rabbit anti-PRAF2 antibodies (1/500 dilution). For light-microscopy experiments, pre-incubation and incubation baths were supplemented with 0.2% Triton X-100. After extensive washing in PBS-BSA, sections were incubated for 1 h with the anti-rabbit IgG (H+L) antibody coupled to Alexa-594 (Invitrogen, France, 1/500 dilution). Sections were then washed in PBS, transferred onto glass slides, and mounted in Mowiol (Sigma, France).

Electron microscopy with peroxidase staining. Immunocytochemistry was performed on free-floating sections. Sections were pre-incubated for 30 min at room temperature in PBS-

BSA and then incubated for 12 h at room temperature with anti-PRAF2 antibodies (1/500 dilution). After extensive washing in PBS-BSA, sections were incubated for 1 h with the biotinylated anti-rabbit IgG (Vector, Burlingame, CA, 1/200 dilution). Sections were then washed in PBS and incubated for 1 h with the avidin-biotinylated-peroxidase complex (Vector) diluted (1/200) in PBS. After a 10-min wash in 0.05 M Tris-HCl, pH7.4, sections were incubated in the same buffer supplemented with 0.03% (w/v) 3,3-diaminobenzidine (Sigma, France) and 0.01% (v/v) hydrogen peroxide. The reaction proceeded at room temperature under light microscope control and was stopped after 5–10 min of incubation by washing in Tris buffer. Sections were incubated in 2.5% glutaraldehyde in PB, rinsed with the same buffer and incubated for 1 h with 2% osmium tetroxide in PB. They were dehydrated in a series of ethanol and flat embedded in epoxy resin (EPON 812 Polysciences). After polymerization, blocks were cut at 70 nm thickness, picked up in 200 mesh cupper grids and observed directly, without staining, under electron microscope.

Electron microscopy with immuno-gold staining. Mice were perfused transcardially with a solution containing 4% paraformaldehyde and 0.1% glutaraldehyde in 0.1 M PB, pH 7.4. After perfusion, brains were removed from the skulls, and immersed in the same fixative for 12 h at 4°C. Tissue blocks were washed in 0.1 M PB and sectioned (vibratome) into coronal sections of 50 µm. Sections were cryo-protected in 20% sucrose in 0.1M PB, freeze-thawed in isopentane and liquid nitrogen. Samples were post-fixed in 2.5 % glutaraldehyde in 0.1 M PB for 20 min, washed and incubated with 2% osmium tetroxide in PB for 20 min. Samples were dehydrated in a series of ethanol and flat embedded in epoxy resin (EPON 812 Polysciences). After polymerization, blocks were cut at 70 nm thickness using an ultramicrotome (Ultracut E Leica) with a diamond knife, picked up on formvar-coated 200 mesh nickel grids. For etching resin and remove osmium, sections were treated with saturated aqueous sodium periodate ($NaIO_4$). They were then immunostained as described (Slot and Geuze 2007), by indirect

immunolabeling with protein gold as immunomarker. Protein A-gold probes (20 nm) were obtained from CMC Utrecht (Netherlands). After immunolabeling, the sections were double stained with uranyl acetate and lead citrate. Control immuno-stainings were performed, in which the primary antibody was omitted. Under these conditions, no selective labeling was observed. Electron microscopic images of the tissue were obtained using a digital camera (Gatan Orius) interfaced with a transmission electron microscope (Philips CM100).

Immunofluorescence analysis. Confocal microscopy and image analysis were performed at the Institut du Fer-à-Moulin Imaging Facility. Sequential labeled images from each region of interest were obtained using laser-scanning confocal microscopy (Olympus Fluoview). To assess the overall level of immunoreactivity in a specific brain area, the optical density of the area was measured with image-J: 100µm diameter circles were acquired for each regions of interest, the acquisition of at least two circles (up to 20 circles for the largest areas) being used to assess the level of immunoreactivity in a specific zone. Immunoreactivity was scored as negative (−), very low (+), low (++), moderate (+++), dense (++++), depending of the mean OD value obtain for each nucleus. Brain structures were defined according to the mouse brain atlas in stereotaxic coordinates from Keith B. J. Franklin and George Paxinos (second edition).

Results:

The specificity of PRAF2 antibodies was assessed in immunohistochemistry and western blot assays (Fig. 1). Confirming the specificity of the PRAF2 antibody, immunostaining was abolished by preabsorption of the antibody with the blocking peptide on mouse brain slices (Fig. 1A). The antibody was characterized further by immunoblotting after sodium dodecyl sulfate-polyacrylamide gel electrophoresis (SDS-PAGE) on total HEK cells membrane preparations, transfected with PRAF1-V5, PRAF2-V5 or PRAF3-V5 constructs (Fig. 1B). In stringent SDS-containing lysis buffer, the PRAF2 antibody recognized a ≈17-kDa molecular species (arrow), consistent with the expected molecular weight of endogenous PRAF2 and a ≈21-kDa molecular species (arrowhead), consistent with the expected molecular weight of PRAF2-V5 (Fig. 1B, upper panel). In HEK cells transfected with PRAF1-V5 or PRAF3-V5 constructs, the PRAF2 antibody only recognize the endogenous PRAF2 (Fig. 1B, upper panel). The peptide-blocked PRAF2 antibody did not recognize PRAF2 or PRAF2-V5, confirming the specificity of this antibody (Fig. 1B, middle panel). As expected, the V5 epitope-directed antibody only recognized PRAF1-V5, PRAF2-V5 and PRAF3-V5 (Fig. 1B, lower panel). Moreover, in a series of immunoblot experiments on rat hippocampal neurons, the signal associated with the anti-PRAF2 antibody was markedly inhibited in extracts from neurons transfected with a PRAF2-specific siRNA compared to control neurons (Doly et al. 2015).

Immunohistochemical experiments were then performed, to investigate the distribution of PRAF2, on coronal sections at various levels of the rostrocaudal axis of mouse CNS. The general expression pattern of PRAF2, previously described in the human brain (Koomoa et al. 2008) was confirmed in mice. PRAF2 was strongly expressed in Purkinje cells and less expressed in molecular and granular layers of mouse cerebellum. In the cerebral cortex and

hippocampus, PRAF2 protein was also detected in neurons, but not in non-neuronal cells. A detailed description of PRAF2 expression is provided below and summarized in Table 1 where the relative labeling intensities of cell body and neuropil immunoreactivity were analyzed: labeling was scored as negative (-), very low (+), low (++), moderate (+++), dense (++++) or very dense (+++++).

Main olfactory bulb

In olfactory bulbs, strong PRAF2 immunoreactivity was present in the mitral cell layer, contrasting with the sparse labeling of neuronal cell bodies in the external plexiformis glomerular, internal plexiformis and granule layers (Fig. 2A). PRAF2 is also expressed in the anterior olfactory nucleus (Fig. 2B), but not in the accessory olfactory bulb (not shown).

Cerebral cortex and Basal ganglia

In the cerebral cortex, PRAF2 immunoreactivity was mainly detected in layers II and V (Fig. 2,3). Only scattered cell body immunostaining were observed in the other laminae, with the exception of an intense band of cell body staining in the deepest part of lamina VI (Fig. 3C). Strong immunolabeling was present in the piriform cortex, compared to other cortical regions (Fig. 3A,C). No immunolabeling was found in basal ganglia such as the nucleus accumbens the globus pallidus and the caudate-putamen (Fig. 3), either in neuronal cell bodies or neuropili (Fig. 3B), contrasting with a strong, almost exclusively cellular, labeling in the endopiriform nucleus (Fig. 3C).

Hippocampus, Amygdala and habenula

In the hippocampus, PRAF2 immunoreactivity was found in the pyramidal layer of the CA1–3 field and in the granular layer of the dentate gyrus (Fig. 4A,B,C). Scattered immunoreactivity was present in the hilus of the dentate gyrus, the strata oriens and radiatum of the CA1-3 field (Fig. 4C). Among the various sub-nuclei of the amygdala, the highest intensity of PRAF2 labeling was found in the basomedial, medial and lateral amygdaloid

nuclei (Fig. 4B). Dense labeling was observed in the medial habenula but only scattered neuronal cell body staining was found in the other nuclei, including the lateral habenula nucleus (Fig. 4B).

Thalamus

Surprisingly, only some sub-nuclei of the thalamus were labeled with the anti-PRAF2 antibody, despite the fact that this area expresses high levels of the GB1 subunit (Bowery et al. 1987; Calver et al. 2000; Charles et al. 2003; Charles et al. 2001; Margeta-Mitrovic et al. 1999; Ulrich et al. 2007). Among the thalamic nuclei, we found the highest immunoreactivity in the anterodorsal and the reticular nuclei (Fig. 4A,B); a moderate level of immunostaining was present in the paratenial laterodorsal and paraventricular nuclei (Fig. 3 and 4A,B). Interestingly, at higher magnification, the labeling pattern of the cell bodies was different between the anterodorsal thalamic nucleus and the pyramidal layer of the hippocampus: an intense punctate immunoreactivity in the former contrasted with a diffuse staining in the latter (Fig. 4A,B).

Midbrain

In the midbrain, the most noticeable labeling was found in the ventral tegmental area and in the substantia nigra pars compacta. Only a weak staining was present in the colliculus, or the periaqueductal gray and oculomotor nuclei (Fig. 5,6). In the ventral tegmental area, some neuronal cell bodies exhibited the same punctate pattern of PRAF2 expression, as in the anterodorsal thalamic nucleus (Fig. 5D).

Pons and Cerebellum

Intense PRAF2 immunoreactivity was found in pontine nuclei, locus coeruleus and pontine raphe nuclei (Fig. 6A,B). In the cerebellum, PRAF2 immunoreactivity was weak in the granule cell layer, the molecular layer and undetectable in white matter-rich areas. Most labeled cell bodies were concentrated in the Purkinje cells layer (Fig. 6B).

Medulla oblongata

Intense cellular staining could be observed in the midline raphe nuclei (Fig. 6A). Some nuclei of the medulla oblongata, such as cochlear, facial, external cuneate, spinal trigeminal, lateral reticular and cuneate nuclei contained highly immunoreactive cell bodies (Fig. 6B,C,D,E and Fig. 7). Scattered cell body immunoreactivity was present in the ambiguus and the gigantocellular reticular nuclei, whereas diffuse staining of neuropili was found in the solitary tract nucleus, the area postrema, and the inferior olive subnucleus. Intense punctate immunoreactivity could be observed in cell bodies of the medulla (Fig. 7A).

Spinal cord

In the spinal cord, the most intense PRAF2 immunoreactivity was observed in the ventral horn at all spinal levels (Fig. 8). In lamina VIII-IX, the cell bodies of presumably large motoneurons were intensely stained, whereas in round smaller-size neurons, presumably interneurons, the staining was much weaker. Some immunoreactive neurons were also distributed around the central canal of lamina X at all spinal levels. Labeling in the dorsal horn was more diffuse and could not be easily attributed to any cell compartment.

Subcellular distributions

The localization of PRAF2 at the subcellular level was then investigated by electron microscopy in the VTA. In these experiments PRAF2 immunoreactivity appeared under the form of either electron-dense amorphous DAB reaction products or gold particles.

PRAF2 was present in axon terminals, identified by the presence of synaptic vesicles (Fig. 9 black star). Both gold particles and DAB products were found at the edge of synaptic vesicles (black arrows) or in mitochondria (m) present in the terminals (Fig. 9A,B,H,I). PRAF2 immunoreactivity was also present in the postsynaptic region of axo-somatic (arrow head in Fig. 9A,B,G) or axo-dendritic contacts (arrow head in Fig. 9D,F,G). Both asymmetric (Fig.

9A,B,D,F,G) and symmetric (Fig. 9C,E) synapses (arrow head) were stained, suggesting that PRAF2 is expressed in excitatory and inhibitory synapses, respectively.

In the cytoplasm, gold particles or DAB products were principally associated with rough endoplasmic reticulum (RER). Among the other cellular organelles, which appear to contain PRAF2 after immunoperoxidase or immunogold staining, there are mitochondria, the cis-Golgi apparatus, nuclei, lysosomes and primary cilia.

In the RER, labeling was mainly found in cisternae, at the cytosolic interface, either under the form of single gold particles, or as aggregates (Fig. 9A,E and Fig. 10D). In smooth endoplasmic reticulum, lacking attached ribosomes, labeling was mostly found at the membrane. PRAF2 also appeared associated with tubulo-vesicular structures.

In mitochondria, the labeling was on both membranes, each of them being well stained by DAB; the immunostaining of the inner membrane extended to the cristae (Fig. 9B,C,D). Gold particles were observed in the internal cristae and also associated with the external membrane (Fig. 9I). In the Golgi apparatus gold particles or DAB products were associated with both cisternae and vesicles: particles were more frequently present in cisternae neighboring RER elements (likely the cis-Golgi) (Fig. 10E,F). In nuclei, the immunoperoxidase staining was observed at the level of the nuclear envelope, with a strong labeling of the nuclear pores (Fig. 11A), the heterochromatin, nucleoli and Cajal bodies (Fig. 11B). Immunostaining was present in both leaflets of the nuclear membrane, which is in continuation with the RE. Gold particles were visible in the nucleoplasm associated to heterochromatin and in nucleoli. In lysosomes immunogold labeling was found in dense matrix or located at the cytosolic side of the lysosomal membrane (Fig. 11C).

Discussion:

Consistent with its function of GB1 gatekeeper (Doly et al. 2015), PRAF2 was present in brain areas expressing the $GABA_B$, including the cortex, the hippocampus, the VTA and raphe nuclei (Charles et al. 2003; Charles et al. 2001; Fritschy et al. 2004; Kulik et al. 2003; Margeta-Mitrovic et al. 1999). PRAF2 expression perfectly matched the distribution of GB1 in these areas. It is likely that in the zones that also express the GB2 subunit (Charles et al. 2001; Clark et al. 2000; Kulik et al. 2003), the actual concentration of cell surface $GABA_B$ is controlled by the relative amount of PRAF2 and GB2. Consistent with our previous observation that moderate changes of PRAF2 expression in the VTA induce hyperactivity in mice (Doly et al. 2015), the unbalanced expression of these proteins would perturb $GABA_B$ receptivity and potentially produce pathological effects. For example, PRAF2 appears to be expressed, as the $GABA_B$, in the pyramidal and granular layers of the hippocampus (Margeta-Mitrovic et al. 1999), a brain area involved in the processing of drug reinforcement behaviors. Preclinical studies have implicated $GABA_B$ receptors in the rewarding effects of drugs of abuse and $GABA_B$ agonists can decrease alcohol withdrawal symptoms in humans and rats (Colombo et al. 2004; Maccioni and Colombo 2009). Moreover, a recent transcriptomic study in postmortem hippocampi found a significant reduction of PRAF2 transcripts in alcoholic patients compared to controls (Enoch et al. 2013), and previous studies demonstrated that PRAF2 controls $GABA_B$ function in primary hippocampal neurons (Doly et al. 2015). Overall, these findings suggest that PRAF2 regulates $GABA_B$ function in these areas and might participate in $GABA_B$-dependent neurological disorders.

In other brain areas PRAF2 expression did not matched perfectly that of GB1. For example, in the spinal cord only motoneurons of the ventral horn were strongly labeled with PRAF2 antibody, whereas the expression of GB1 and GB2 subunits was well documented in both the dorsal and the ventral horn (Charles et al. 2001; Margeta-Mitrovic et al. 1999), suggesting

that $GABA_B$ function in the dorsal horn is not controlled by PRAF2.

The absence of detectable PRAF2 expression in basal ganglia (caudate putamen, globus palidus, nucleus accumbens) or hypothalamic neurons is particularly appealing, since these brain areas also express small amounts of GB2 subunits comparatively to GB1 (Burman et al. 2003; Calver et al. 2000; Clark et al. 2000; Durkin et al. 1999; Ng and Yung 2001). Interestingly, despite low GB2 expression, physiological functions attributable to GB1 were documented in these nuclei (Chen and Yung 2004; Lux-Lantos et al. 2008). Previous studies showed that reconstituted cell systems or neurons lacking the GB2 subunit could nevertheless express functional, although often atypical, GB1-containing GABA receptors (Baloucoune et al. 2012; Gassmann et al. 2004; Kaupmann et al. 1997; Richer et al. 2009). In these situations, the unbalanced expression of GB1 over that of PRAF2 may overload the PRAF2-mediated ER retention, thereby allowing a fraction of GB1 to reach the cell surface despite the absence of GB2 and somehow couple to G-proteins. In this context, the atypical responses elicited by GB1 activation (Gassmann et al. 2004) might proceed via alternative coupling of GB1 homo-dimers or from the heterodimerization of GB1 with other GPCRs co-expressed in the same neurons.

Strong PRAF2 expression was found in some brain areas expressing no or low levels of GB1, such as cuneate, gracile and lateral reticular nuclei, suggesting that PRAF2 might control the export of other GPCRs or other types of plasma membrane proteins in the CNS. Although, $GABA_B$ receptors are the prototypical model of intracellularly-retained GPCRs with regulated cell-surface export, several other GPCRs undergo similar regulated trafficking from ER or Golgi stores (Achour et al. 2008). In particular, PRAF2 was reported to interact with the chemokine receptor CCR5 (Schweneker et al. 2005) and preliminary Bioluminescence Resonance Energy Transfer (BRET) and co-IP experiments indicated that PRAF2 can

associate with other chemokine receptors, such as CCR2 and CCR7, and with 5-HT2 serotoninergic receptors (unpublished data).

Previous fluorescence microscopy studies indicated that PRAF2 was mostly co-localized with ER markers (Doly et al. 2015). However, in hippocampal neurons, a fraction of PRAF2 was consistently found co-localized with a cis-Golgi marker and additional protein did not co-localize with either marker. The electron microscopy study confirmed the presence of PRAF2 in additional organelles or structures. Some PRAF2 was expressed in presynaptic vesicles and in the postsynaptic density. This finding is reminiscent of previous studies on PRAF1 and PRAF3, showing that both proteins were also located in the synaptic area and could interact with specific synaptic proteins, such as VAMP2, synaptophysin, synuclein and piccolo (Akiduki et al. 2007; Fenster et al. 2000; Lee et al. 2011; Martincic et al. 1997). Moreover, PRAF2 was found in synaptic vesicles preparations from rat brain (Koomoa et al. 2008). Altogether, these observations suggest that PRAF2 might play a role in the regulation of the synaptic function through the control of the vesicular trafficking or docking of GPCRs or other membrane-associated proteins. Although not investigated so far, PRAF2 might regulate the plasma membrane translocation of some specific Rab protein in the presynaptic (Rab3/5) or postsynaptic (Rab8/5) area (Ng and Tang 2008).

Some PRAF2 labeling was present at the nuclear membrane, nuclear pores and nucleoli, consistent with the presence of PRAF2 in nuclei and perinuclear regions of neuroblastoma cells and in the nuclear fraction of U-87 malignant glioma cells (Borsics et al. 2010; Geerts et al. 2007). To date, there is no evidence for a nuclear function of PRAF2. However, Yip3p, the yeast homologue of PRAF1 was reported to interact with RTN1p reticulon (Geng et al. 2005), whereas PRAF2 interacts with RTN4, also known as the neurite outgrowth inhibitor Nogo (Vento et al. 2010). Reticulons are membrane-associated proteins involved in cell trafficking, inhibition of axonal growth, and apoptosis (Chiurchiu et al. 2014; Yang and Strittmatter

2007). Interestingly, RTN4A also localizes to subdomains of the nuclear envelope and its inhibition by anti-RTN4A antibodies limits nuclear envelope assembly (Kiseleva et al. 2007). PRAF2/RTN4 interaction might thus play a role in nuclear envelope maintenance or in the localization of protein partners in this compartment.

The localization of PRAF2 in the mitochondria of midbrain neurons is consistent with the observation that PRAF2 and PRAF3 can interact with both Bcl-2 and Bcl-xL (Vento et al. 2010). Whereas Bcl-2, is predominantly localized in the ER, Bcl-xL is mainly a mitochondrial outer membrane protein (Kaufmann et al. 2003). PRAF2 overexpression induces the translocation and the aggregation of Bax in mitochondria, increasing caspase activity and cell death. As a pro-survival member of the Bcl-2 familly, Bcl-xL plays a unique role in the general resistance to cytotoxic agents. In neurons, it also stimulates synapse formation, increases mitochondrial fission and fusion and modulates exchange of metabolites across the outer mitochondrial membrane (Berman et al. 2009; Li et al. 2008; Vander Heiden et al. 2001). Pro-apoptotic Bcl-2 family members, such as Bax, regulate programmed cell death in neurons (Krajewski et al. 1994; Oltvai et al. 1993). Bax and Bcl-xL are expressed in midbrain dopaminergic neurons and were implicated in trauma response and Parkinson disease (Anderton et al. 2012; Horowitz et al. 2003; Shim et al. 2004; van der Heide and Smidt 2013; Vila and Przedborski 2003). PRAF2 might control Bcl-xl and Bax localization in the RE or mitochondria of midbrain neurons, the impaired sorting of these proteins potentially leading to neurodegeneration or neural death after brain injury. PRAF2-dependent perturbation of the pro and anti-apoptotic equilibrium, trough BAX and Bcl-xL relocation, might play a role in cancer genesis or progression (Borsics et al. 2010; Fo et al. 2006; Geerts et al. 2007; Vento et al. 2010; Yco et al. 2013).

A previously non-documented specific localization of PRAF2 is the primary cilium. However this finding is consistent with the result of a genomic screen aimed at identifying

ciliogenesis modulators (Kim et al. 2010). In this study siRNA-induced PRAF2 knockdown was reported to facilitate ciliogenesis and primary cilium extension. Interestingly, all PRAF members might participate in ciliogenesis regulation: PRAF1 was identified in a proteomic analysis of the cilium complex (Liu et al. 2007); PRAF3 interacts with the Arf-like GTPase ARL6, which is implicated in the regulation of ciliary transport and recruitment of the BBS (Bardet-Biedl Syndrome) complex, a group of proteins involved in genetic ciliopathies (Fan et al. 2004). The molecular mechanisms of PRAF2-dependent regulation of ciliogenesis and cilium extension have not been investigated so far but might involve the capacity of PRAF2 to regulate GPCRs. Indeed, primary cilia are enriched in some GPCRs, such as the somatostatin receptor 3 (Sstr3) (Handel et al. 1999), the serotonin receptor 6 (5-HT6r) (Brailov et al. 2000), the melanin-concentrating hormone receptor 1 (Mchr1) (Berbari et al. 2008a) and the dopamine receptor 1 (D1r) (Domire et al. 2011). Interestingly, BBS proteins are required for Sstr3 and Mchr1 localization in cilia (Berbari et al. 2008b) and impaired GPCR targeting to cilia can cause learning and memory defects or hyperphagia-induced obesity (Berbari et al. 2008b; Davenport et al. 2007; Einstein et al. 2010). In conclusion, PRAF2 might play either direct or indirect role, via its interacting partners, in the relocalization or trafficking of GPCRs to primary cilia.

In summary, PRAF2 appeared widely distributed in various regions of the CNS, from the olfactory bulbs to the spinal cord. PRAF2 expression was particularly dense in brain regions previously shown to contain the GB1 subunit of the $GABA_B$ receptor but other areas exist where GB1 and PRAF2 expression do not overlap. These finding suggest that $GABA_B$ function is not exclusively controlled by PRAF2 and, on the other hand, that PRAF2 might control the export of other membrane-associated proteins in the CNS. At the subcellular level, several other organelles contain PRAF2 in addition to the RE anticipating additional functions that remain to be elucidated.

Conflict of Interest: The authors declare that they have no conflict of interest.

Figure Legends:

Fig.1: **Specificity of the PRAF2 antibody.**

A: Confocal scanning fluorescent micrographs of the midbrain and spinal cord (C1) immuno-labeled with the rabbit polyclonal PRAF2 antibody are shown before and after pre-absorption with the immunizing peptide at a 5:1 ratio of peptide to antibody protein (w/w). PRAF2 immunostaining was abolished by pre-absorption of the antibody with the antigen. B: Western immunoblot analysis of total lysate from HEK-293 cells, transfected with PRAF1-V5, PRAF2-V5 or PRAF3-V5 constructs, using the mouse monoclonal V5 antibody or PRAF2 antibody (with or without blocking Peptide). Arrow: endogenous expression of PRAF2 in HEK293 cells. Arrowhead: PRAF2-V5 expression. Stereotaxic coordinates, upper panel, Bregma -3,08mm. Scale bars: 1mm

Fig.2: **Distribution of PRAF2 immunoreactivity in the olfactory bulb (A), frontal cortex and the anterior olfactory nucleus (B)**

(a) and (b) correspond to enlarged area of the respective insets in each panel. Abbreviations: M2: secondary motor cortex, AOV: anterior olfactory nucleus ventral part, Pir: piriform cortex, Prl: prelimbic cortex, MO: medial orbital cortex, Mi: Mitral cell layer of the olfactory bulb, GCL: Granule cell layer, EPL: external plexiform layer, Gl: glomerular layer of the olfactory bulb, aci: anterior commissure intrabulbar part, Io: inferior olive. Scale bars: 1mm. Inset scale bars: 100µm. Stereotaxic coordinates: Bregma +4mm (A), Bregma +2,46mm (B).

Fig.3: **Lack of PRAF2 immunoreactivity in the nucleus accumbens and caudate-putamen (A,B) and distribution of PRAF2 immunoreactivity in the parietal and piriform cortex (A,C)**

(a) and (b) correspond to enlarged area of the respective insets in panel B. Abbreviations: CPu: caudate putamen, AcbC: accumbens nucleus core, AcbSh: accumbens nucleus shell, Cp: corpus callosum, LGP: lateral globus pallidus, BST: bed nucleus of the stria terminalis, PVA: paraventricular thalamic nucleus, LH: lateral hypothalamic area, Den: dorsal endopiriform nucleus, aca: anterior commissure anterior part, Par: parietal cortex, Pir: Piriform cortex . Scale bars 1mm. Inset scale bars: 100µm. Stereotaxic coordinates: Bregma +1,4mm (A), Bregma -0,4mm (C).

Fig.4: **Distribution of PRAF2 immunoreactivity in the anterodorsal thalamic nucleus (A), hippocampus, amygdala and the habenula (B,C)**

(a) and (b) correspond to enlarged area of the respective insets for each panel. Abbreviations: DG: dentate gyrus, MePD: medial amygdaloid nucleus posterodorsal part, MHb: medial habenular nucleus, Den: dorsal endopiriform nucleus, BM: basomedial amygdaloid nucleus, LHb: lateral habenular nucleus, Rt: reticular thalamic nucleus, LH: lateral hypothalamic area, VMH: ventromedial hypothalamic nucleus, Pyr: pyramidal cells, GCL: granule cell layer, H: hilus, ML: molecular layer, PVA: paraventricular thalamic nucleus, AD: anterodorsal thalamic nucleus, VPM: ventral posteromedial thalamic nucleus, VL: ventrolateral nucleus, sm: stria medullaris thalamus, Rad: stratum radiatum, Or: strata oriens. Scale bar: 1mm. Inset (a) scale bar: 100µm. Insets (b) scale bars: 10µm. Stereotaxic coordinates: Bregma -1,14mm (A), Bregma -2,25mm (B).

Fig.5 : **Distribution of PRAF2 immunoreactivity in the lateral mammillary nuclei (A), substantia nigra compacta and ventral tegmental area (B,C). PRAF2 immunoreactivity in cell bodies of VTA neurons (D)**

(a) Correspond to enlarged area of the respective inset in panel A. Abbreviations: PAG: Periaqueductal gray, DG: dentate gyrus, MG: medial geniculate nucleus, LH: lateral hypothalamic area, VTA: ventral tegmental area, SNC: substancia nigra compacta, MM: medial mammillary nucleus, SNR: substantia nigra pars reticulata, Zo: zonal layer of superior colliculus, LM: lateral mammillary nucleus, PMCo: posteromedial cortical amygdaloid nucleus. Scale bar: 1mm. Scale bar (D): 10µm. Inset (a) scale bar: 100µm. Stereotaxic coordinates: Bregma -2,94mm (A), Bregma -3,08mm (B), Bregma -3,14mm (C).

Fig.6 : **Distribution of PRAF2 immunoreactivity in the periaqueductal gray, dorsal and median raphe nucleus (A), the facial nucleus, hypoglossal nucleus, cerebellum (B) and the spinal trigeminal nucleus (C,D,E)**

(a) and (b) correspond to enlarged area of the respective insets in panel A. Abbreviations: MVePC: medial vestibular nucleus parvicellular part, Amb: ambiguus nucleus, Pn: pontine nuclei, IP: Interpeduncular nucleus, PFl: paraflocculus, Med: medial fastigial cerebellar nucleus, DC: dorsal cochlear nucleus, VCP: ventral cochlear nucleus posterior part, 7N : facial nucleus, Gi: gigantocellular reticular nucleus, Ecu: external cuneate nucleus, PAG Periaqueductal gray, DR dorsal raphe nucleus, MnR: median raphe nucleus, ML molecular layer, GR: granular cells layer, Pur: purkinje cells layer, 12N: hypoglossal nucleus, 10cb: 10th Cerebellar lobule, Sp5: spinal trigeminal nucleus. Scale bar: 1mm. Inset scale bars: 100µm. Stereotaxic coordinates: Bregma -4,48mm (A), Bregma -6,08mm (B), Bregma -6,94mm (C), Bregma -7,08mm (D), Bregma -7,56mm (E).

Fig.7 : **Distribution of PRAF2 immunoreactivity in the cuneate nucleus (A), lateral reticular nucleus, hypoglosal nucleus (B) and the gracile nucleus (C)**

(a) and (b) correspond to enlarged area of the respective insets in each panel. Abbreviations: Sol: Nucleus of the solitary tract, 10N: dorsal motor nucleus of vagus, 12N: hypoglossal nucleus, Sp5: spinal trigeminal nucleus, cu: cuneate fasciculus, Cu: cuneate nucleus, LRt: lateral reticular nucleus, IOC: inferior olive subnucleus C, MdV: medullary reticular nucleus ventral part, AP: area postrema, Gr: gracile nucleus. Scale bar: 1mm. Inset (a) scale bars: 100µm. Inset (b) scale bar: 10µ

m Stereotaxic coordinates: Bregma -7,64mm (A), Bregma -8mm (B).

Fig.8 : **Distribution of PRAF2 immunoreactivity in the cervical (C2-C6), thoracic (T1), lumbar (L2, L5) and sacral (S2) spinal cord**

Abbreviations: DH: dorsal horn, VH: ventral horn. Scale bar: 1mm

Fig.9: **PRAF2 is express in post and presynaptic terminals of the VTA**

A, B: PRAF2 immunoperoxidase staining is present in axo-somatic contacts. PRAF2 is readily detected as a dark amorphous, diaminobenzidine (DAB) reaction product, staining the vesicles (arrows) and mitochondria (m) enclosed in the axon terminal(*). Labeling was also observed in postsynaptic contacts (arrowheads). The neuronal soma display labeling in mitochondria, the rough endoplasmic reticulum (RER), lysosomes (ly) and multivesicular bodies (mvb). C, D: Axo-dendritic contacts forming symmetric (C) and asymmetric (D) contacts with PRAF2 immunostaining in vesicles (arrow) and mitochondria (m). In postsynaptic dendrites the labeling was found in mitochondria (m) and tubulo-vesicular elements (double arrows). E: Labeling is present in an axo-somatic contact neighboring an

immunoperoxidase labeled primary cilia (arrow). In the neuronal soma, mitochondria and RER are also immunostained. F, G: PRAF2 immunoperoxidase staining is present in axo-dendritic (F) and axo-somatic (G) contacts at the postsynaptic level (arrowheads). In these cases, pre-synaptic terminals are not labeled (*). F: the presence of labeled RER elements in dendritic compartment (white arrows) argue in favor of the spiny nature of the dendrite. Example of non labeled synapse (black arrow) in (G). H, I: Gold particles labeling in axon terminal (*) contacting neuronal soma (H) or dendrite (I). Immunoparticles appeared at the edges of synaptic vesicles. I: example of symmetric (black arrow head) and asymmetric (white arrow head) synapse

Fig.10: **PRAF2 distribution in the neuronal soma of the VTA**

A: Nuclei (N) showing DAB immunoreaction in the nuclear envelope. Immunostaining is also present in nuclear pores (arrowheads). B: Gold particles labeling, the nuclear envelope (arrow) RER element (double arrows) and Golgi apparatus (AG). C: Immunoperoxidase staining is present in the endoplasmic reticulum deriving from the nuclear envelope (arrow). D: Gold particles can be seen associated with RER cisternae (arrowhead), being enclosed or located at their surface. E, F: Immunostaining in the cis-Golgi apparatus (arrowhead) and RER cisternae (arrows). The trans-Golgi apparatus is less frequently labeled

Fig.11: **PRAF2 expression in the nucleus, lysosome and primary cilium**

A: PRAF2 Immunoperoxidase staining in the nucleus (N) showing the labeling at the nuclear pores (arrowheads) and in heterochromatin. B: Immunostaining is present in the granular component of the nucleoli (n) and in condensed chromatin (arrowheads). C: lysosomes (arrowheads) are densely stained in the dense matrix. Low (D) and high (E) magnification of

a labeled primary cilium (arrow). Plasma membrane around the cilia is also labeled (arrowhead)

Achour L, Labbe-Juillie C, Scott MGH, Marullo S (2008) An escort for G Protein Coupled Receptors to find their path: implication for regulation of receptor density at the cell surface. Trends Pharmacol Sci 29:528-535

Akiduki S, Ikemoto MJ (2008) Modulation of the neural glutamate transporter EAAC1 by the addicsin-interacting protein ARL6IP1 J Biol Chem 283:31323-31332 doi:10.1074/jbc.M801570200

Akiduki S, Ochiishi T, Ikemoto MJ (2007) Neural localization of addicsin in mouse brain Neurosci Lett 426:149-154 doi:10.1016/j.neulet.2007.08.056

Anderton RS et al. (2012) Co-regulation of survival of motor neuron and Bcl-xL expression: implications for neuroprotection in spinal muscular atrophy Neuroscience 220:228-236 doi:10.1016/j.neuroscience.2012.06.042

Baloucoune GA et al. (2012) GABAB receptor subunit GB1 at the cell surface independently activates ERK1/2 through IGF-1R transactivation PLoS One 7:e39698 doi:10.1371/journal.pone.0039698

Benke D (2010) Mechanisms of GABAB receptor exocytosis, endocytosis, and degradation Adv Pharmacol 58:93-111 doi:10.1016/S1054-3589(10)58004-9

Berbari NF, Johnson AD, Lewis JS, Askwith CC, Mykytyn K (2008a) Identification of ciliary localization sequences within the third intracellular loop of G protein-coupled receptors Mol Biol Cell 19:1540-1547 doi:10.1091/mbc.E07-09-0942

Berbari NF, Lewis JS, Bishop GA, Askwith CC, Mykytyn K (2008b) Bardet-Biedl syndrome proteins are required for the localization of G protein-coupled receptors to primary cilia Proc Natl Acad Sci U S A 105:4242-4246 doi:10.1073/pnas.0711027105

Berman SB et al. (2009) Bcl-x L increases mitochondrial fission, fusion, and biomass in neurons J Cell Biol 184:707-719 doi:10.1083/jcb.200809060

Bjork S, Hurt CM, Ho VK, Angelotti T (2013) REEPs are membrane shaping adapter proteins that modulate specific g protein-coupled receptor trafficking by affecting ER cargo capacity PLoS One 8:e76366 doi:10.1371/journal.pone.0076366

Borsics T, Lundberg E, Geerts D, Koomoa DL, Koster J, Wester K, Bachmann AS (2010) Subcellular distribution and expression of prenylated Rab acceptor 1 domain family, member 2 (PRAF2) in malignant glioma: Influence on cell survival and migration Cancer Sci 101:1624-1631 doi:10.1111/j.1349-7006.2010.01570.x

Bowery NG, Hudson AL, Price GW (1987) GABAA and GABAB receptor site distribution in the rat central nervous system Neuroscience 20:365-383

Brailov I, Bancila M, Brisorgueil MJ, Miquel MC, Hamon M, Verge D (2000) Localization of 5-HT(6) receptors at the plasma membrane of neuronal cilia in the rat brain Brain Res 872:271-275

Brock C, Boudier L, Maurel D, Blahos J, Pin JP (2005) Assembly-dependent surface targeting of the heterodimeric GABAB Receptor is controlled by COPI but not 14-3-3 Mol Biol Cell 16:5572-5578

Burman KJ et al. (2003) GABAB receptor subunits, R1 and R2, in brainstem catecholamine and serotonin neurons Brain Res 970:35-46

Caddick SJ, Hosford DA (1996) The role of GABAB mechanisms in animal models of absence seizures Mol Neurobiol 13:23-32 doi:10.1007/BF02740750

Calver AR et al. (2000) The expression of GABA(B1) and GABA(B2) receptor subunits in the cNS differs from that in peripheral tissues Neuroscience 100:155-170

Charles KJ, Calver AR, Jourdain S, Pangalos MN (2003) Distribution of a GABAB-like receptor protein in the rat central nervous system Brain Res 989:135-146

Charles KJ, Evans ML, Robbins MJ, Calver AR, Leslie RA, Pangalos MN (2001) Comparative immunohistochemical localisation of GABA(B1a), GABA(B1b) and GABA(B2) subunits in rat brain, spinal cord and dorsal root ganglion Neuroscience 106:447-467

Chen L, Yung WH (2004) GABAergic neurotransmission in globus pallidus and its involvement in neurologic disorders Sheng Li Xue Bao 56:427-435

Chiurchiu V, Maccarrone M, Orlacchio A (2014) The role of reticulons in neurodegenerative diseases Neuromolecular Med 16:3-15 doi:10.1007/s12017-013-8271-9

Clark JA, Mezey E, Lam AS, Bonner TI (2000) Distribution of the GABA(B) receptor subunit gb2 in rat CNS Brain Res 860:41-52

Colombo G et al. (2004) Role of GABA(B) receptor in alcohol dependence: reducing effect of baclofen on alcohol intake and alcohol motivational properties in rats and amelioration of alcohol withdrawal syndrome and alcohol craving in human alcoholics Neurotox Res 6:403-414

Crunelli V, Leresche N (1991) A role for GABAB receptors in excitation and inhibition of thalamocortical cells Trends Neurosci 14:16-21

Davenport JR et al. (2007) Disruption of intraflagellar transport in adult mice leads to obesity and slow-onset cystic kidney disease Curr Biol 17:1586-1594 doi:10.1016/j.cub.2007.08.034

Doly S, Marullo S (2015) Gatekeepers controlling GPCR export and function Trends in Pharmacological Sciences doi:10.1016/j.tips.2015.06.007

Doly S et al. (2015) GABA receptor cell-surface export is controlled by an endoplasmic reticulum gatekeeper Mol Psychiatry doi:10.1038/mp.2015.72

Domire JS, Green JA, Lee KG, Johnson AD, Askwith CC, Mykytyn K (2011) Dopamine receptor 1 localizes to neuronal cilia in a dynamic process that requires the Bardet-Biedl syndrome proteins Cell Mol Life Sci 68:2951-2960 doi:10.1007/s00018-010-0603-4

Durkin MM, Gunwaldsen CA, Borowsky B, Jones KA, Branchek TA (1999) An in situ hybridization study of the distribution of the GABA(B2) protein mRNA in the rat CNS Brain Res Mol Brain Res 71:185-200

Einstein EB et al. (2010) Somatostatin signaling in neuronal cilia is critical for object recognition memory J Neurosci 30:4306-4314 doi:10.1523/JNEUROSCI.5295-09.2010

Enoch MA, Baghal B, Yuan Q, Goldman D (2013) A factor analysis of global GABAergic gene expression in human brain identifies specificity in response to chronic alcohol and cocaine exposure PLoS One 8:e64014 doi:10.1371/journal.pone.0064014

Fan Y et al. (2004) Mutations in a member of the Ras superfamily of small GTP-binding proteins causes Bardet-Biedl syndrome Nat Genet 36:989-993 doi:10.1038/ng1414

Fenster SD et al. (2000) Piccolo, a presynaptic zinc finger protein structurally related to bassoon Neuron 25:203-214

Ferrarelli F, Tononi G (2011) The thalamic reticular nucleus and schizophrenia Schizophr Bull 37:306-315 doi:10.1093/schbul/sbq142

Fo CS, Coleman CS, Wallick CJ, Vine AL, Bachmann AS (2006) Genomic organization, expression profile, and characterization of the new protein PRA1 domain family, member 2 (PRAF2) Gene 371:154-165 doi:10.1016/j.gene.2005.12.009

Fritschy JM, Sidler C, Parpan F, Gassmann M, Kaupmann K, Bettler B, Benke D (2004) Independent maturation of the GABA(B) receptor subunits GABA(B1) and GABA(B2) during postnatal development in rodent brain J Comp Neurol 477:235-252 doi:10.1002/cne.20188

Gassmann M et al. (2004) Redistribution of GABAB(1) protein and atypical GABAB responses in GABAB(2)-deficient mice J Neurosci 24:6086-6097 doi:10.1523/JNEUROSCI.5635-03.2004

Geerts D, Wallick CJ, Koomoa DL, Koster J, Versteeg R, Go RC, Bachmann AS (2007) Expression of prenylated Rab acceptor 1 domain family, member 2 (PRAF2) in neuroblastoma: correlation with clinical features, cellular localization, and cerulenin-mediated apoptosis regulation Clin Cancer Res 13:6312-6319 doi:10.1158/1078-0432.CCR-07-0829

Geng J, Shin ME, Gilbert PM, Collins RN, Burd CG (2005) Saccharomyces cerevisiae Rab-GDI displacement factor ortholog Yip3p forms distinct complexes with the Ypt1 Rab GTPase and the reticulon Rtn1p Eukaryot Cell 4:1166-1174 doi:10.1128/EC.4.7.1166-1174.2005

Handel M et al. (1999) Selective targeting of somatostatin receptor 3 to neuronal cilia Neuroscience 89:909-926

Horowitz JM, Pastor DM, Goyal A, Kar S, Ramdeen N, Hallas BH, Torres G (2003) BAX protein-immunoreactivity in midbrain neurons of Parkinson's disease patients Brain Res Bull 62:55-61

Hutt DM, Da-Silva LF, Chang LH, Prosser DC, Ngsee JK (2000) PRA1 inhibits the extraction of membrane-bound rab GTPase by GDI1 J Biol Chem 275:18511-18519 doi:10.1074/jbc.M909309199

Inoue K, Akiduki S, Ikemoto MJ (2005) Expression profile of addicsin/GTRAP3-18 mRNA in mouse brain Neurosci Lett 386:184-188 doi:10.1016/j.neulet.2005.06.013

Jankowski MM et al. (2013) The anterior thalamus provides a subcortical circuit supporting memory and spatial navigation Front Syst Neurosci 7:45 doi:10.3389/fnsys.2013.00045

Kaufmann T, Schlipf S, Sanz J, Neubert K, Stein R, Borner C (2003) Characterization of the signal that directs Bcl-x(L), but not Bcl-2, to the mitochondrial outer membrane J Cell Biol 160:53-64 doi:10.1083/jcb.200210084

Kaupmann K et al. (1997) Expression cloning of GABA(B) receptors uncovers similarity to metabotropic glutamate receptors Nature 386:239-246 doi:10.1038/386239a0

Kaupmann K et al. (1998) GABA(B)-receptor subtypes assemble into functional heteromeric complexes Nature 396:683-687 doi:10.1038/25360

Kim J et al. (2010) Functional genomic screen for modulators of ciliogenesis and cilium length Nature 464:1048-1051 doi:10.1038/nature08895

Kiseleva E, Morozova KN, Voeltz GK, Allen TD, Goldberg MW (2007) Reticulon 4a/NogoA locates to regions of high membrane curvature and may have a role in nuclear envelope growth J Struct Biol 160:224-235 doi:10.1016/j.jsb.2007.08.005

Koomoa DL, Go RC, Wester K, Bachmann AS (2008) Expression profile of PRAF2 in the human brain and enrichment in synaptic vesicles Neurosci Lett 436:171-176 doi:10.1016/j.neulet.2008.03.030

Krajewski S, Krajewska M, Shabaik A, Miyashita T, Wang HG, Reed JC (1994) Immunohistochemical determination of in vivo distribution of Bax, a dominant inhibitor of Bcl-2 Am J Pathol 145:1323-1336

Kulik A, Vida I, Lujan R, Haas CA, Lopez-Bendito G, Shigemoto R, Frotscher M (2003) Subcellular localization of metabotropic GABA(B) receptor subunits GABA(B1a/b) and GABA(B2) in the rat hippocampus J Neurosci 23:11026-11035

Lee HJ, Kang SJ, Lee K, Im H (2011) Human alpha-synuclein modulates vesicle trafficking through its interaction with prenylated Rab acceptor protein 1 Biochem Biophys Res Commun 412:526-531 doi:10.1016/j.bbrc.2011.07.028

Li H et al. (2008) Bcl-xL induces Drp1-dependent synapse formation in cultured hippocampal neurons Proc Natl Acad Sci U S A 105:2169-2174 doi:10.1073/pnas.0711647105

Lin CI, Orlov I, Ruggiero AM, Dykes-Hoberg M, Lee A, Jackson M, Rothstein JD (2001) Modulation of the neuronal glutamate transporter EAAC1 by the interacting protein GTRAP3-18 Nature 410:84-88 doi:10.1038/35065084

Liu Q et al. (2007) The proteome of the mouse photoreceptor sensory cilium complex Mol Cell Proteomics 6:1299-1317 doi:10.1074/mcp.M700054-MCP200

Lux-Lantos VA, Bianchi MS, Catalano PN, Libertun C (2008) GABA(B) receptors in neuroendocrine regulation Cell Mol Neurobiol 28:803-817 doi:10.1007/s10571-008-9263-4

Maccioni P, Colombo G (2009) Role of the GABA(B) receptor in alcohol-seeking and drinking behavior Alcohol 43:555-558 doi:10.1016/j.alcohol.2009.09.030

Maier PJ, Zemoura K, Acuna MA, Yevenes GE, Zeilhofer HU, Benke D (2014) Ischemia-like oxygen and glucose deprivation mediates down-regulation of cell surface γ-aminobutyric acidB receptors via the endoplasmic reticulum (ER) stress-Induced transcription factor CCAAT/enhancer-binding protein (C/EBP)-homologous protein (CHOP). J Biol Chem 289:12896-12907 doi:10.1074/jbc.M114.550517

Margeta-Mitrovic M, Mitrovic I, Riley RC, Jan LY, Basbaum AI (1999) Immunohistochemical localization of GABA(B) receptors in the rat central nervous system J Comp Neurol 405:299-321

Martincic I, Peralta ME, Ngsee JK (1997) Isolation and characterization of a dual prenylated Rab and VAMP2 receptor J Biol Chem 272:26991-26998

Ng EL, Tang BL (2008) Rab GTPases and their roles in brain neurons and glia Brain Res Rev 58:236-246 doi:10.1016/j.brainresrev.2008.04.006

Ng TK, Yung KK (2001) Differential expression of GABA(B)R1 and GABA(B)R2 receptor immunoreactivity in neurochemically identified neurons of the rat neostriatum J Comp Neurol 433:458-470

Oltvai ZN, Milliman CL, Korsmeyer SJ (1993) Bcl-2 heterodimerizes in vivo with a conserved homolog, Bax, that accelerates programmed cell death Cell 74:609-619

Pfeffer S, Aivazian D (2004) Targeting Rab GTPases to distinct membrane compartments Nat Rev Mol Cell Biol 5:886-896 doi:10.1038/nrm1500

Richer M et al. (2009) GABA-B(1) receptors are coupled to the ERK1/2 MAP kinase pathway in the absence of GABA-B(2) subunits J Mol Neurosci 38:67-79 doi:10.1007/s12031-008-9163-6

Schweneker M, Bachmann AS, Moelling K (2005) JM4 is a four-transmembrane protein binding to the CCR5 receptor FEBS Lett 579:1751-1758 doi:10.1016/j.febslet.2005.02.037

Shim JW et al. (2004) Enhanced in vitro midbrain dopamine neuron differentiation, dopaminergic function, neurite outgrowth, and 1-methyl-4-phenylpyridium resistance in mouse embryonic stem cells overexpressing Bcl-XL J Neurosci 24:843-852 doi:10.1523/JNEUROSCI.3977-03.2004

Slot JW, Geuze HJ (2007) Cryosectioning and immunolabeling Nat Protoc 2:2480-2491 doi:10.1038/nprot.2007.365

Ulrich D, Besseyrias V, Bettler B (2007) Functional mapping of GABA(B)-receptor subtypes in the thalamus J Neurophysiol 98:3791-3795 doi:10.1152/jn.00756.2007

van der Heide LP, Smidt MP (2013) The BCL2 code to dopaminergic development and Parkinson's disease Trends Mol Med 19:211-216 doi:10.1016/j.molmed.2013.02.003

Vander Heiden MG, Li XX, Gottleib E, Hill RB, Thompson CB, Colombini M (2001) Bcl-xL promotes the open configuration of the voltage-dependent anion channel and metabolite passage through the outer mitochondrial membrane J Biol Chem 276:19414-19419 doi:10.1074/jbc.M101590200

Vento MT, Zazzu V, Loffreda A, Cross JR, Downward J, Stoppelli MP, Iaccarino I (2010) Praf2 is a novel Bcl-xL/Bcl-2 interacting protein with the ability to modulate survival of cancer cells PLoS One 5:e15636 doi:10.1371/journal.pone.0015636

Vila M, Przedborski S (2003) Targeting programmed cell death in neurodegenerative diseases Nat Rev Neurosci 4:365-375 doi:10.1038/nrn1100

Wyss JM, Swanson LW, Cowan WM (1979) A study of subcortical afferents to the hippocampal formation in the rat Neuroscience 4:463-476

Yang YS, Strittmatter SM (2007) The reticulons: a family of proteins with diverse functions Genome Biol 8:234 doi:10.1186/gb-2007-8-12-234

Yco LP, Geerts D, Koster J, Bachmann AS (2013) PRAF2 stimulates cell proliferation and migration and predicts poor prognosis in neuroblastoma Int J Oncol 42:1408-1416 doi:10.3892/ijo.2013.1836

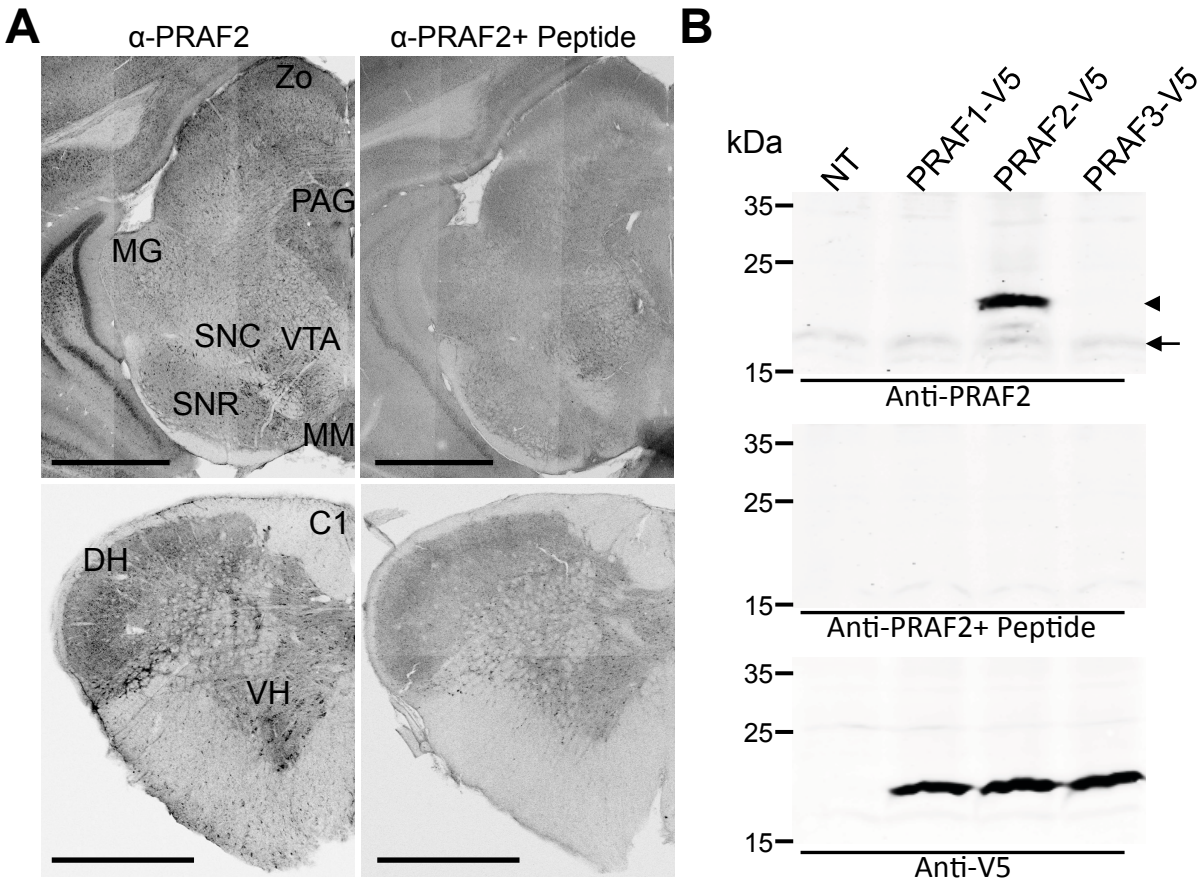
A
α-PRAF2
α-PRAF2+ Peptide
Zo
PAG
MG
SNC
VTA
SNR
MM
C1
DH
VH
B
kDa
NT
PRAF1-V5
PRAF2-V5
PRAF3-V5
35
25
15
Anti-PRAF2
Anti-PRAF2+ Peptide
Anti-V5

Figure 1

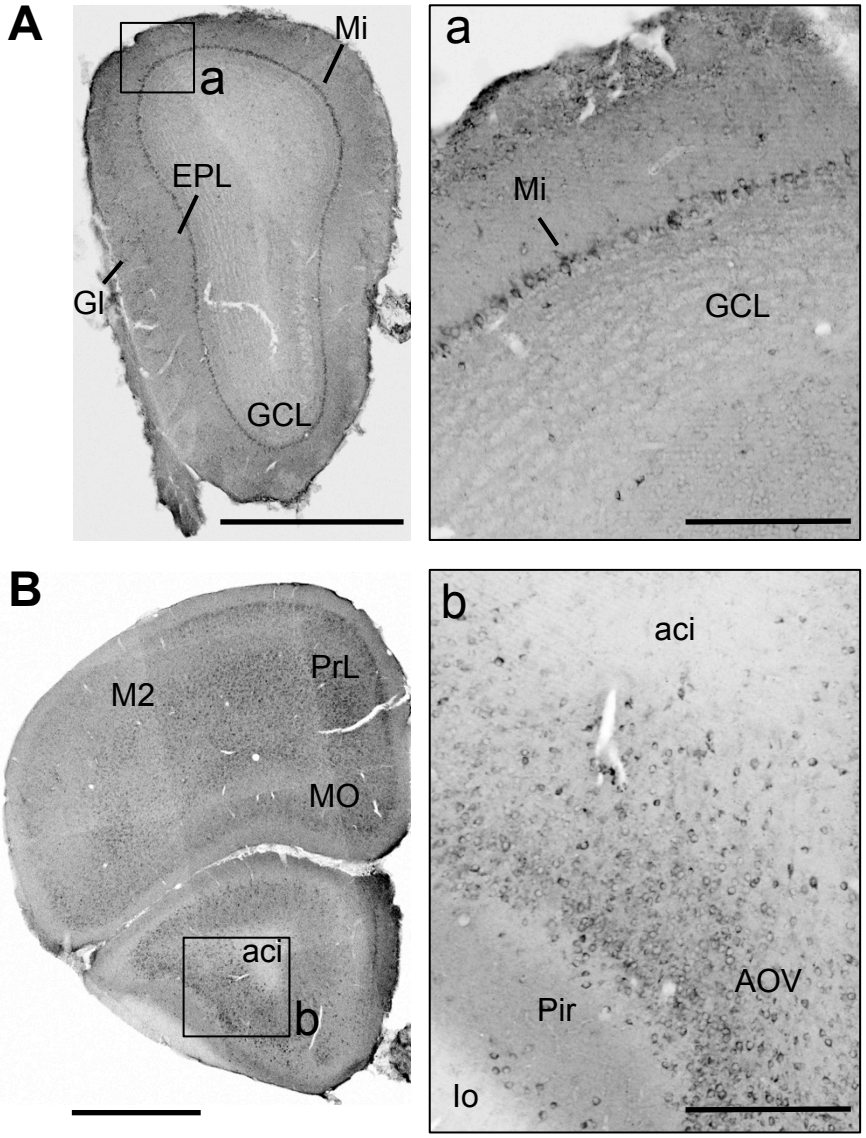

Figure 2

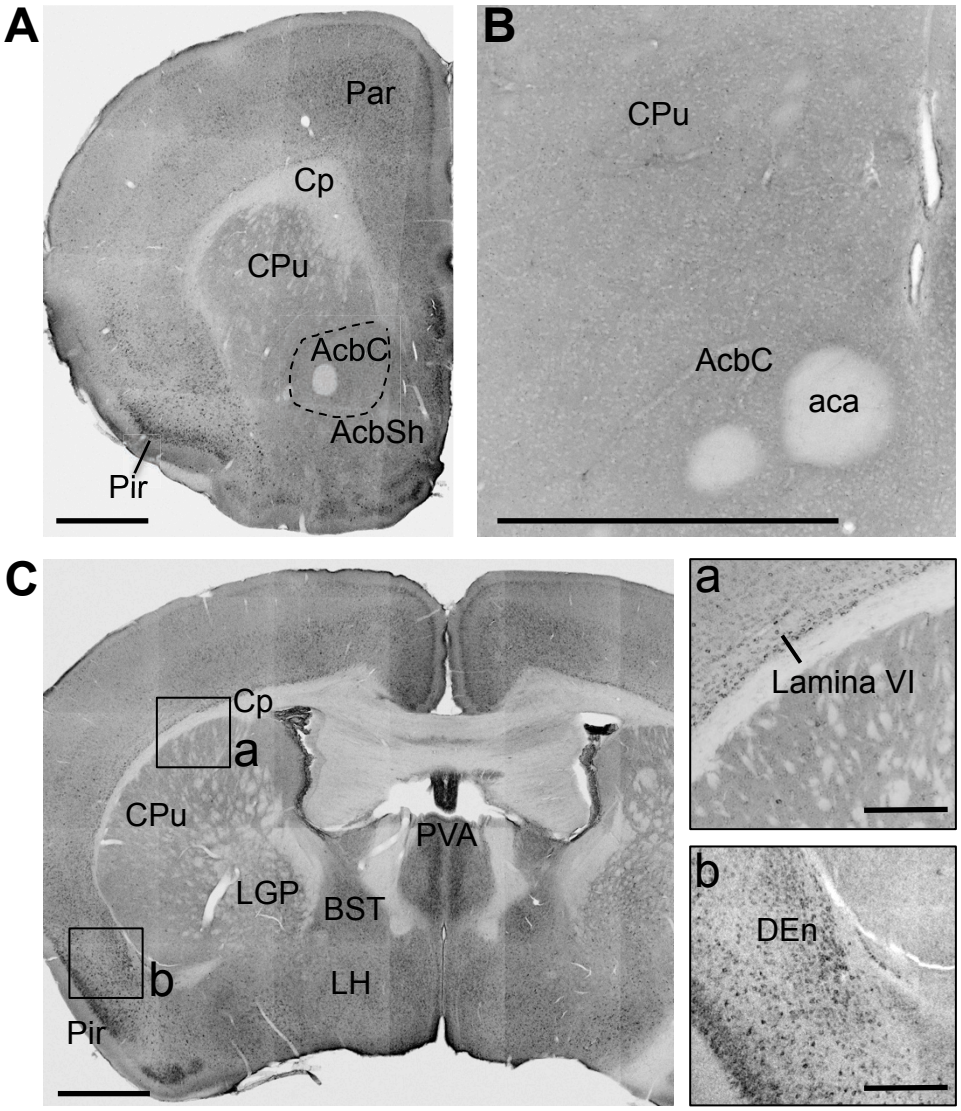
A
Par
Cp
CPu
AcbC
AcbSh
Pir
B
CPu
AcbC
aca
C
Cp
a
CPu
PVA
LGP
BST
b
LH
Pir
a
Lamina VI
b
DEn

Figure 3

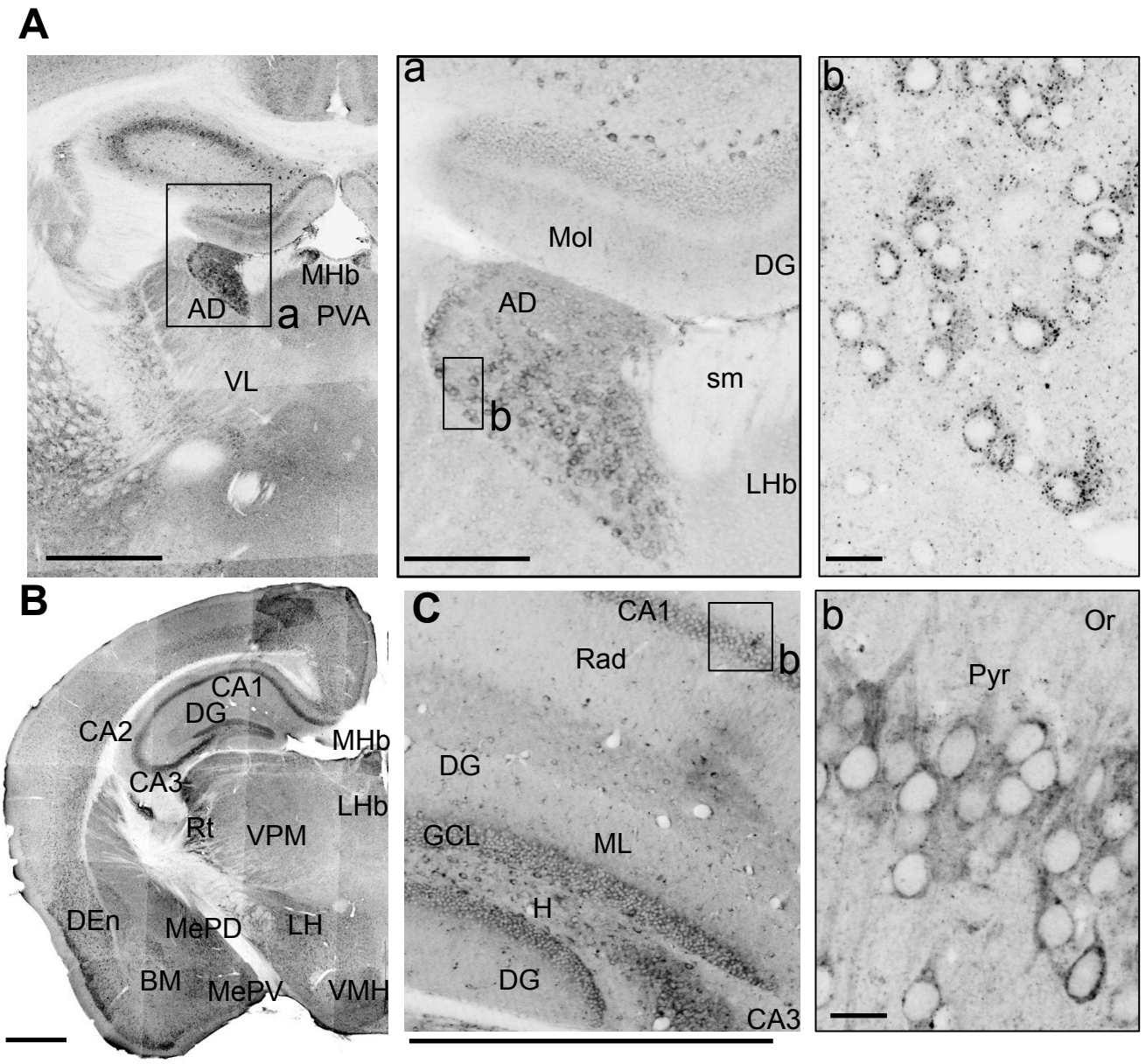
A
MHb
AD
a
PVA
VL
a
Mol
DG
AD
sm
b
LHb
b
B
CA1
DG
CA2
MHb
CA3
LHb
Rt
VPM
DEn
MePD
LH
BM
MePV
VMH
C
CA1
Rad
b
DG
GCL
ML
H
DG
CA3
b
Or
Pyr

Figure 4

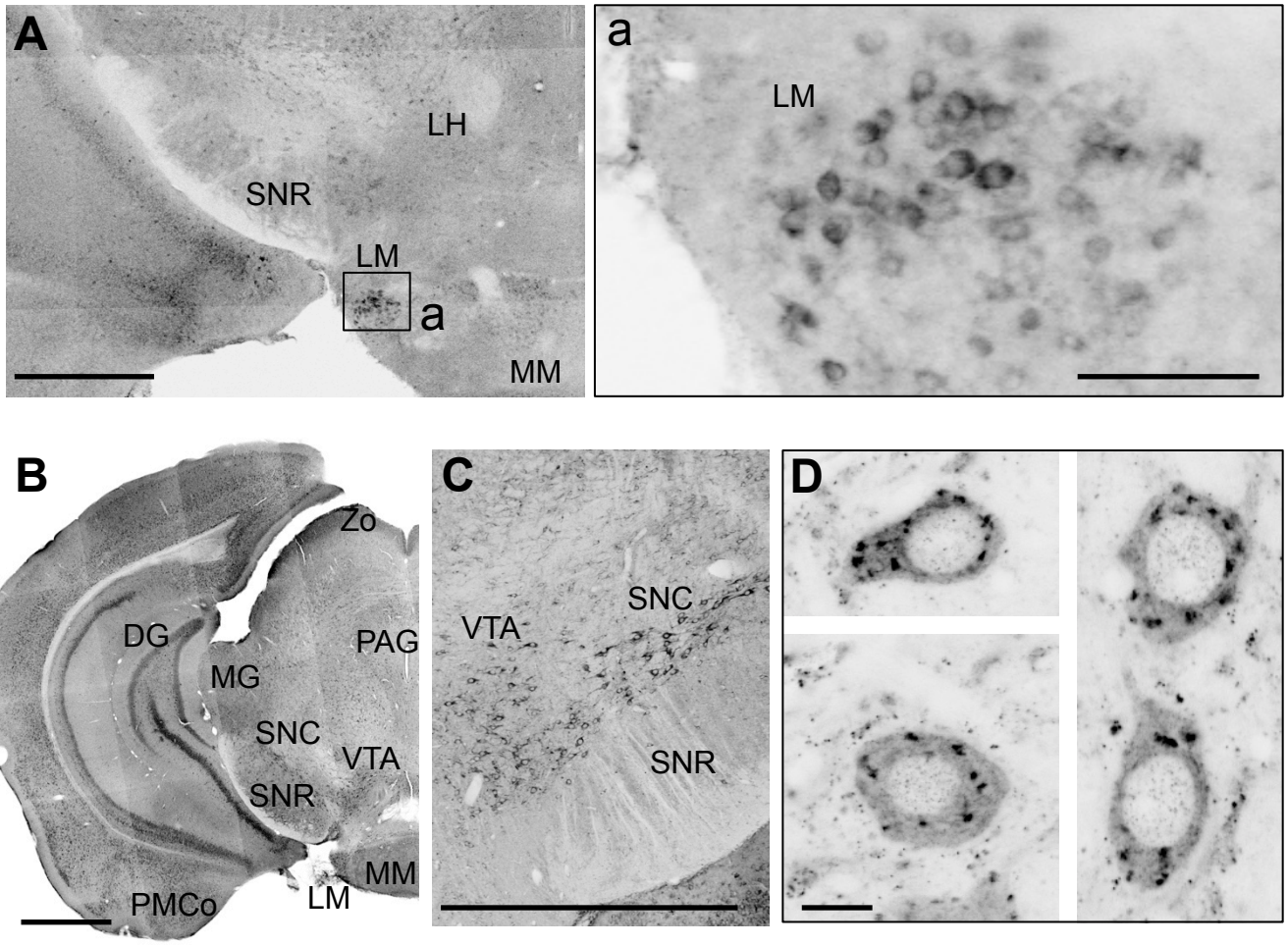
A
LH
SNR
LM
a
MM
a
LM
B
Zo
DG
PAG
MG
SNC
VTA
SNR
MM
PMCo
LM
C
SNC
VTA
SNR
D

Figure 5

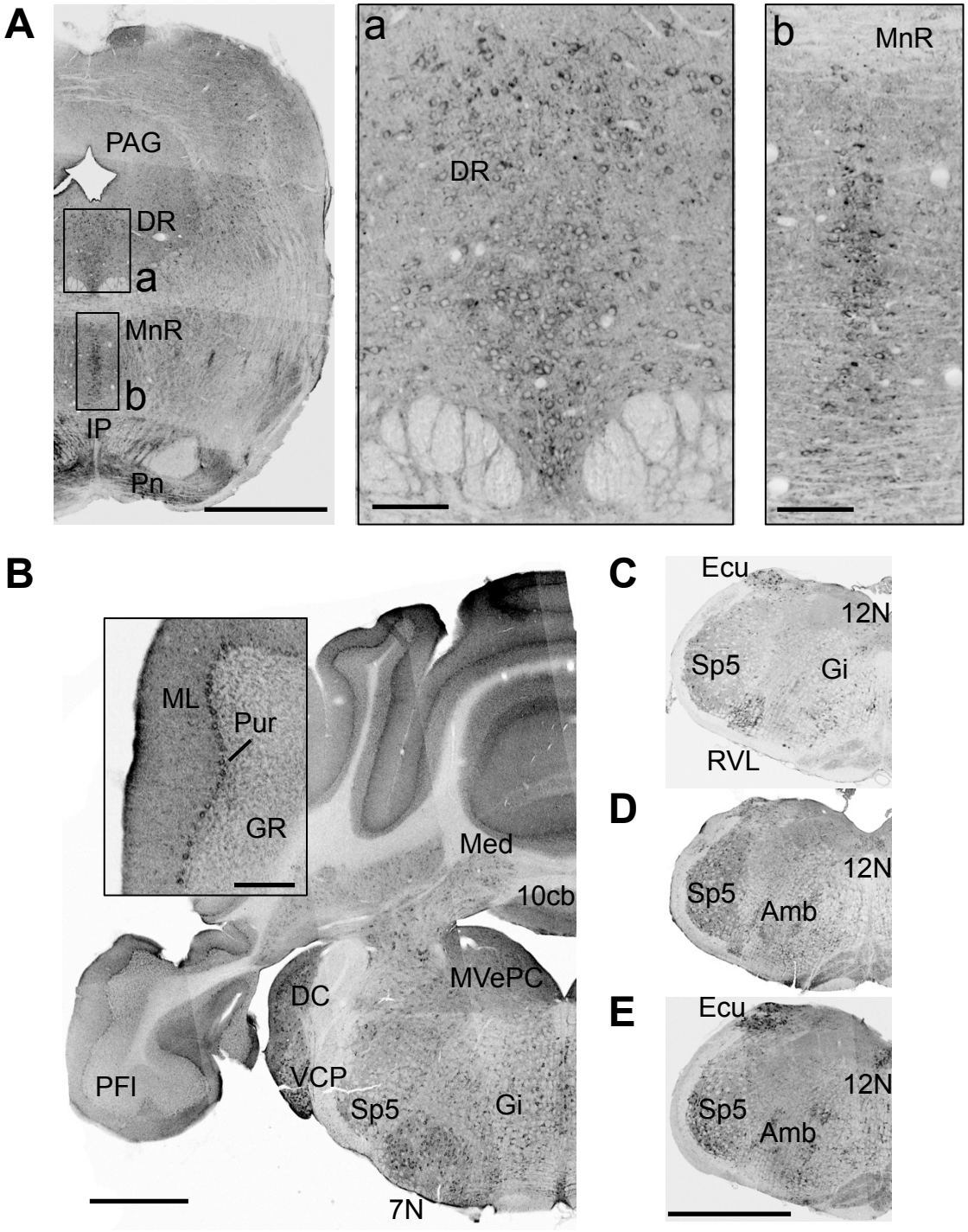
A
PAG
DR
a
MnR
b
IP
Pn
a
DR
b
MnR
B
ML
Pur
GR
Med
10cb
MVePC
DC
PFl
VCP
Sp5
Gi
7N
C
Ecu
12N
Sp5
Gi
RVL
D
12N
Sp5
Amb
E
Ecu
12N
Sp5
Amb

Figure 6

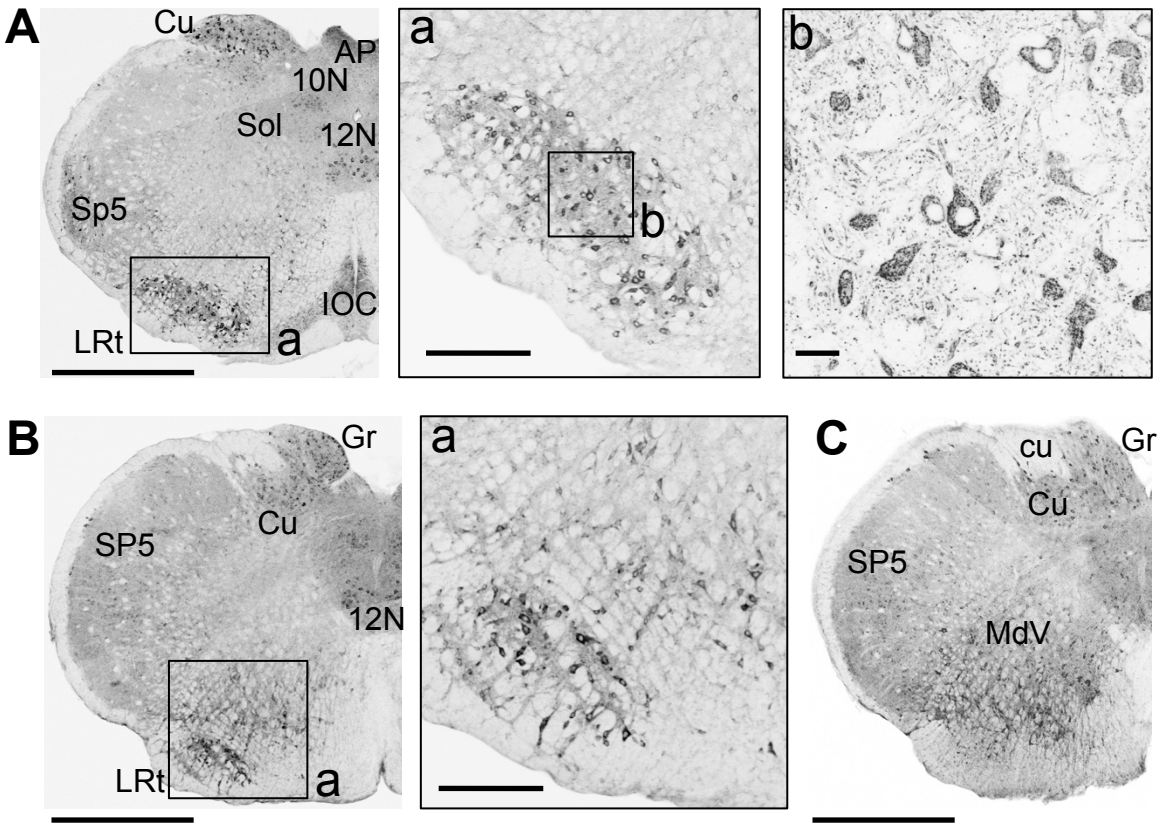
A
Cu
AP
10N
Sol
12N
Sp5
IOC
LRt
a
a
b
b
B
Gr
SP5
Cu
12N
LRt
a
a
C
cu
Gr
Cu
SP5
MdV

Figure 7

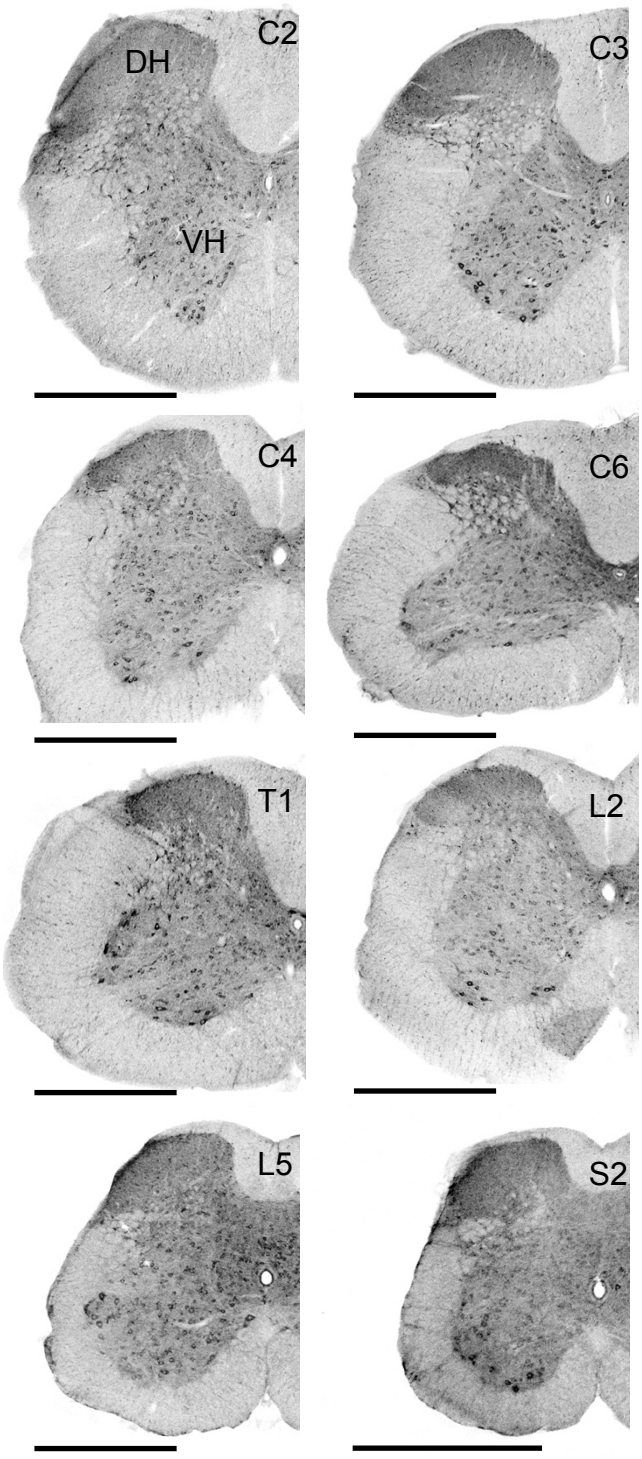

Figure 8

Table 1: Distribution of PRAF2 in the Mouse Central Nervous System

Main olfactory bulb	**Thalamus**	**Pons**
Glomerular layer +	Anterodorsal nucleus ++++	Pontine nuclei +++
External plexiform layer +	Anteroventral nucleus ++	Locus coeruleus +++
Mitral cell layer ++++	Anteromedial nucleus +	Posterodorsal tegmental nucleus +
Granule cell layer -	Paratenial nucleus +++	Dorsomedial tegmental area +
Cerebral Cortex	Laterodorsal nucleus +++	Ventral tegmental nucleus -
Layer I -	Mediodorsal nucleus +++	Pontine reticular nuclei ++
Layer II +++	Paraventricular nucleus +++	Pontine raphe nuclei +++
Layer II I+++	Rhomboid nucleus -	Lateral parabrachial nucleus +++
Layer IV +	Reuniens nucleus -	Medial parabrachial nucleus +
Layer V ++++	Reticular nucleus ++++	Nucleus of the lateral lemniscus -
Layer VI ++	Centrolateral nucleus +	Paralemniscal nucleus +
Piriform ++++	Centromedial nucleus ++	Principal sensory trigeminal nucleus -
Hippocampus	Ventrolateral nucleus +	Motor trigeminal nucleus -
CA1 ++	Ventromedial nucleus -	Paraolivary nucleus ++
CA2 ++	Ventoposterolateral nucleus +	Nucleus of the trapezoid body -
CA3 ++	Ventroposteromedial nucleus -	A5 area +++
Dentate gyrus ++	Posterior nucleus +	Barrington's nucleus +
Subiculum ++	Submedius nucleus -	**Medulla oblongata**
Basal ganglia	Parafascicular nucleus -	Spinal trigeminal nucleus++
Caudate putamen -	**Hypothalamus**	Abducens nucleus +
Nucleus accumbens -	Suprachiasmatic nucleus ++	Facial nucleus ++++
Globus pallidus -	Periventricular nucleus -	medial vestibular nucleus, parvicellular ++++
Endopiriform nucleus +++	Supraoptic nucleus -	medial vestibular nucleus, magnocellular +
Septal and basal forebrain regions	Paraventricular nucleus +	Cochlear nucleus ++++
Lateral septal nucleus -	Median eminence +	Ambiguus nucleus ++
Bed nucleus of the stria terminalis ++	Ventromedial nucleus +++	Nucleus of the solitary tract +++
Subfornical organ -	Arcuate nucleus -	Raphe nuclei ++++
Amygdala	Bed nucleus anterior commissure +	Dorsal motor nucleus of vagus +
Anterior nucleus +	Lateral hypothalamic area +++	Hypoglossal nucleus +++
Posteromedial nucleus +	Posterior hypothalamic area -	Lateral reticular nucleus ++++
Posterolateral nucleus +	Dorsomedial nucleus ++	External cuneate nucleus ++++
Medial amygdaloid nucleus +++	Mammillary nucleus -	Cuneate nucleus ++++
Basomedial amygdaloid nucleus +++	Lateral mammillary nucleus ++++	Gracile nucleus ++++
Lateral amygdaloid nucleus ++	**Midbrain**	Gigantocellular reticular nucleus +++
Basolateral amygdaloid nucleus +	Substantia nigra Pars compacta ++++	Area postrema +++
Central amygdaloid nucleus +	Substantia nigra Pars reticulata ++	**Spinal cord**
Intercalated amygdaloid nuclei +	Ventral tegmental area +++++	Lamina I +
Habenula	Interpeduncular nucleus -	Lamina II ++
Medial nucleus +++	Superior colliculus+	Lamina III -
Lateral nucleus -	Periaqueductal gray ++	Lamina IV +
Cerebellum	Oculomotor nucleus -	Laminae V–VIII ++++
Molecular layer +	Inferior colliculus ++	Lamina IX ++++
Purkinje cell layer ++++	Cuneiform nucleus ++	Lamina X +++
Granule cell layer -	Nucleus of the optic tract ++	

Intensity of PRAF2: +++++, very strong; ++++, strong; +++, moderate; ++, low; +, very low; -, absente

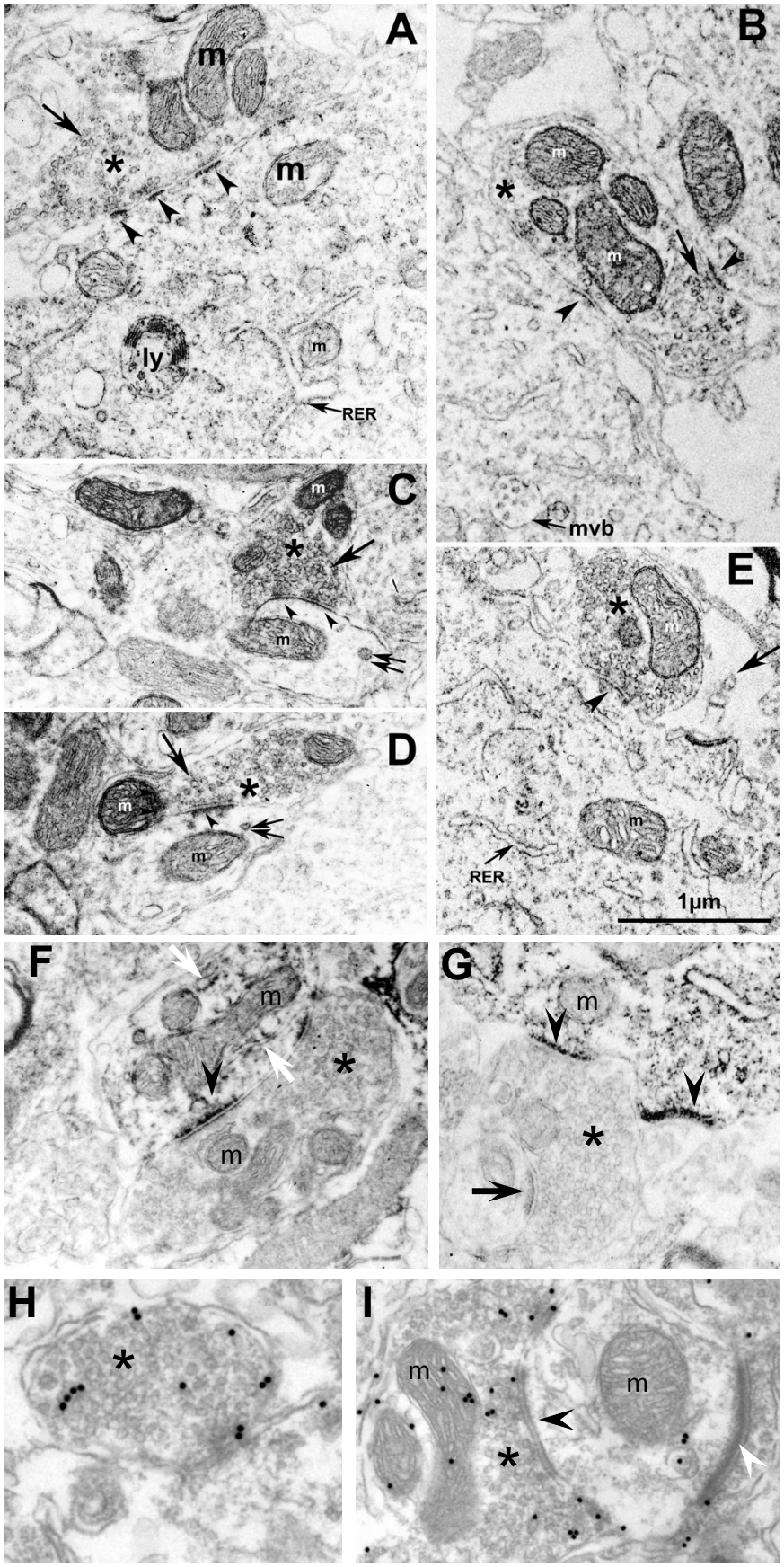

Figure 9

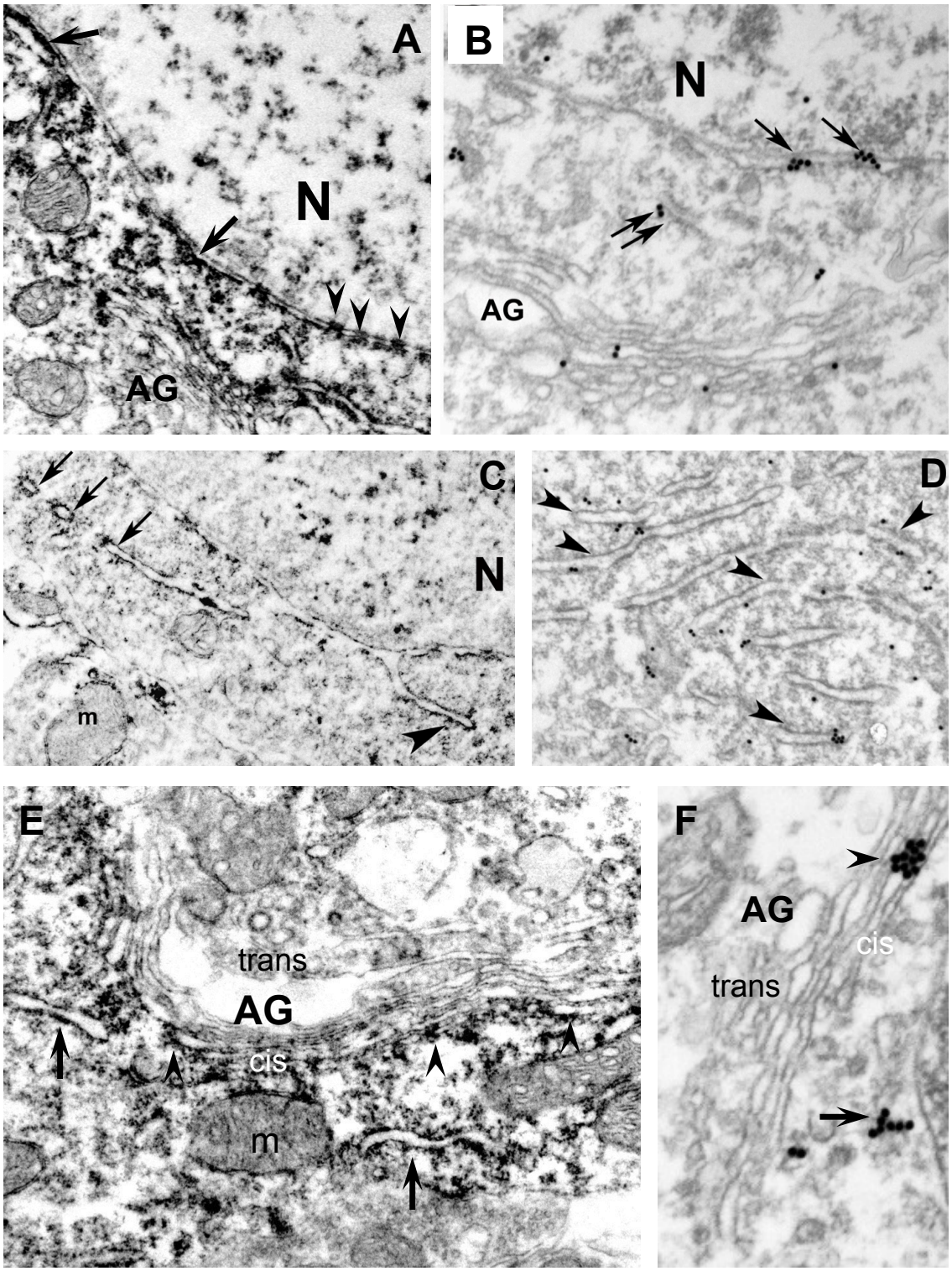

Figure 10

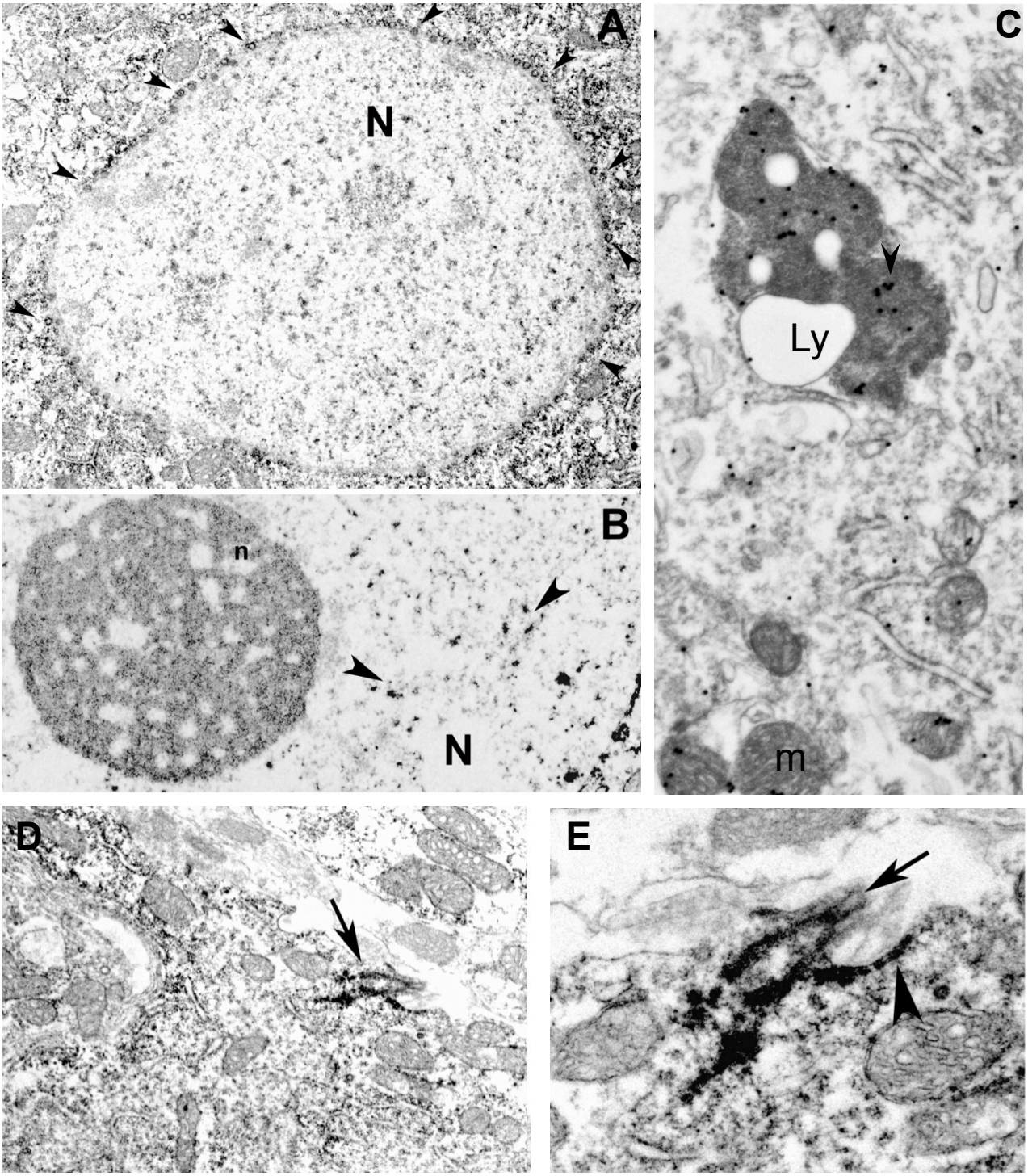

Figure 11